- DRAFT – FEB. 3, 1998 –

Cruise report on North Solomon trench survey, KH-98 Leg 1

January 27, 1998 – January 30, 1998

RV Hakuho Maru
Ocean Research Institute
University of Tokyo

KH98-1 Cruise LEG.1 1998.1.16~2.3 Tokyo-Cairns

Name	Title	Institute	E-mail address
Asahiko Taira (Chief Scientist of the Mission)	Professor	ORI, Univ. of Tokyo	ataira@ori.u-tokyo.ac.jp
Hidekazu Tokuyama	Associate Professor	ORI, Univ. of Tokyo	tokuyama@ori.u-tokyo.ac.jp
Hiroaki Toh	Research Associate	ORI, Univ. of Tokyo	toh@ori.u-tokyo.ac.jp
Kimihiro Mochizuki	Research Associate	ORI, Univ. of Tokyo	kimi@ori.u-tokyo.ac.jp
Masao Nakanishi	Research Associate	ORI, Univ. of Tokyo	nakanisi@ori.u-tokyo.ac.jp
Chiaki Igarashi	Technical Staff	ORI, Univ. of Tokyo	igarashi@ori.u-tokyo.ac.jp
Fujio Yamamoto	Technical Staff	ORI, Univ. of Tokyo	yamamoto@ori.u-tokyo.ac.jp
Eiichiro Araki	Graduate Student	ORI, Univ. of Tokyo	araki@ori.u-tokyo.ac.jp
Shinji Yoneshima	Graduate Student	ORI, Univ. of Tokyo	shinji@ori.u-tokyo.ac.jp
Hiromasa Nishisaka	Graduate Student	Chiba Univ.	nishisaka@earth.s.chiba-u.ac.jp
Manabu Mochida	Graduate Student	Chiba Univ.	mmochida@earth.s.chiba-u.ac.jp
Takashi Yoshizawa	Graduate Student	Chiba Univ.	tyoshiza@earth.s.chiba-u.ac.jp
Yoshiharu Nagaya	Chief Scientist	Hydorgrapic Department, Japan	ynagaya@cue.jhd.go.jp
Wietze Van der Werff	Research Fellow	Geol. Sur. Japan	wietze@gsj.go.jp
Edward L. Winterer	Professor	Scripps Inst. Oceanography	jwinterer@ucsd.edu
Paul Mann	Research Scientist	Univ. of Texas	paulm@utig.ig.utexas.edu

Aker: I have made a few very minor editorial suggestions (in red ink) Jerry Winterer

copies of preprints

TH IPL copy

- DRAFT - FEB. 3, 1998 -

Cruise report on North Solomon trench survey, KH-98-Leg 1

January 27, 1998 - January 30, 1998

RV Hakuho Maru, Ocean Research Institute
University of Tokyo

Tectonic setting and significance of the North Solomon trench

The Solomon island arc has been the focus of seismic, geologic, and marine geophysical surveys over the past 25 years since it was first proposed in the early 1970's that the Solomon arc was the best example of an arc polarity reversal on Earth. As ~~most~~ many ancient arcs are assumed to have reversed polarity during their evolution, the Solomon island arc became a natural laboratory for the study of the deformational and igneous signatures of this fundamental tectonic process.

Early workers proposed a model for entry of the Ontong Java Plateau (OJP) into the North Solomon trench about 10 Ma with subsequent arc polarity reversal and initiation of subduction along the San Cristobal trench on the southwestern edge of the arc (Fig. 1). Because polarity reversal was thought to be completed by about 10 Ma, it was assumed by previous workers that the North Solomon trench is now an extinct trench feature. More recent work on a 1995 Ewing MCS dataset by Phinney (1997) and others has shown that the initial entry of the thickened part of the OJP into the North Solomon trench may have occured as late as 4-2 Ma. Moreover, Phinney (1997) documents abundant evidence for active trench deformation along the length of the North Solomon trench.

The 1995 Ewing survey also revealed the presence of a sub-horizontal decollement within the Cretaceous igneous basement of the OJP that extends to a depth of 7 km beneath the northwestern end (Choiseul structural domain) of the Malaita accretionary prism (Fig. 1). The Choiseul structural domain became an interesting target for further study during KH-

98-1 because:

· The decollement was imaged on only two of the fifteen Ewing MCS lines across the Malaita accretionary prism (lines 26, 28 on Figure 1). Thirteen MCS lines to the southwest exhibited evidence for active trench deformation at shallow levels but no decollement could be traced beneath the trench slope.

· The decollement on Ewing lines 26 and 28 exhibited a blind thrust relationship with nascent trench topography at the northwestern end of the North Solomon trench (Figs. 3, 4). On both lines, the decollement ramps upward at a angle of 20-30 degrees to occupy the center of a seafloor ridge that is on strike with the better developed trench slope of the North Solomon trench to the south.

· The decollement was interpreted by Phinney (1997) as delamination of the upper 7 km of crystalline rock and pelagic cover of the OJP because the large crustal thickness of the OJP (~35 km - Miura et al., 1996) prevented its complete subduction.

· It was postulated that trench deformation of the North Solomon trench is propagating into the Ontong Java plateau from the southeast where the trench is deep and well developed to the northwest in the Choiseul structural domain where the seafloor becomes flat and undisturbed. This direction of propagation is consistent with the more highly deformed structural domains to the southeast of the Choiseul domain and the oblique convergence direction of the Pacific plate (OJP) on the North Solomon trench.

Goals of the KH-98-1 survey

The main goals of the survey were to:

· Use 24 channel multichannel reflection data to better constrain the geometry of the decollement at higher levels in the crust. The 1995 lines did not image the decollement at depths above 5.5 seconds (Figs. 3, 4).

These lines would also be used to focus an ODP drilling proposal to investigate the rates of deformation and physical properties of the decollement at shallow levels.

· Use Izanagi sidescan data to determine the pattern of seafloor faulting and sedimentation in the area of incipient and ongoing trench deformation.

· Use Seabeam data to better constrain the bathymetry of the area.

· Deploy three OBS instruments on the seafloor above the decollement to monitor microseismicity in the range of magnitudes 3.0-4.0 associated with the decollement for a period of about 30 days.

Izanagi, MCS, and Seabeam survey data coverage and relation to 1995 Ewing MCS lines

The map in Figure 2 shows the distribution of MCS, Izanagi and Seabeam lines collected during the three day survey which began on January 27, 1998, to January 30, 1998. For reference, the locations of the 1995 Ewing MCS lines are also shown.

OBS survey. The initial part of the survey was devoted to deployment of 3 OBS instruments (NC1-3) over the area of decollement which was identified on 1995 Ewing lines 26 and 28. The instruments were deployed on either side of Line 28 which is the line showing the presumably youngest part of the decollement. The instruments will be recovered by another ship in early March, 1998.

MCS and Izanagi survey. The second stage in the survey was to deploy the MCS and Izanagi equipment and commence collection of data along Line 1. Lines were oriented at an oblique angle to trench-related structures to maximize their seafloor reflectivity on the Izanagi survey. The close spacing of MCS lines will allow them to become a loose 3-D survey on an interactive workstation that will alleviate problems of interpreting the oblique structural sections. Moreover, the KH-98 MCS lines cross the Ewing MCS lines and could therefore be used to site potential ODP drill sites.

Izanagi background inforamation. The Izanagi system which was introduced to Ocean Research
Institute, the University of Tokyo in 1989, is a deep ocean swath

mapping system. The Izanagi has a long range and is towed at shallow depth, typically 100 m below the sea surface with a speed up to 10 knots (Fig.1). It transmits 11 kHz on the port side and 12 kHz on the starboard side. The three major components of the system are the towfish, launch and recovery system and surface electronics system.The Izanagi towfish is towed behind a depressor in a streamlined, passively stabilized, near neutrally buoyant vehicle. The outgoing signal from each side of the Izanagi towed array is shaped in a beam which is almost 70 degrees wide vertically , but is only about 2.0 degrees wide horizontally (along the survey ship's track).

The system produces real-time acoustic backscattering images down to 10,000 m of water depth and up to 40 km of swath width. The IZANAGI acoustic backscattering images are composed of 1,024 pixels per side of the swath ; thus for a 10 km swath each pixel represents the echo strength from a band at a constant width of 5 m. Monitor records of the acoustic backscattering images are produced on an EPC 8700 variable chart recorder, photographed, reduced in size, and assembled into a mosaic of the seafloor. The Izanagi plots strong reflectors as dark and shadows as light, so the images appear as negatives. In addition,
the system can measure the direction of the reflected signal from the seafloor, so that the bathymetry can be calculated for the ensonified swath of oceanfloor. The Izanagi system generates ~~both~~ both acoustic backscattering images and swath bathymetric maps. Fig. 2 shows a schematic of the Izanagi transducers and acoustic arrival angle geometry. As the transducer spacing is equal to one-half wavelength, phase angle of -180 degrees to +180 degrees are possible. Bathymetry is derived from measurements of the phase difference of echoes received at two transducer rows separated by about half a wavelength in a plane parallel to the face of the corresponding acoustic array. These phase angles are sampled at 4 kHz and binned into a two-dimensional histogram of phase angles versus time after bottom detection. Then phase angles are converted directly to depths and horizontal distances ~~through~~ by running the sonar system over a "known" portion of the seafloor in the vicinity of the survey area. In practise the conversion of measured phase angle to acoustic arrival

angle is determined via flat bottom table. This table, which maps electric angles to acoustic angles, is generated by binning and integrating the phase angle and slant range data collected over a bottom known to be flat.

Izanagi towing configuration and acoustic arrival angle measuring geometry. This information is provided graphically in Figure 5.

MCS data parameters. Acquisition parameters are summarized on Table 1. Specifications of streamer are summarized on Table 2 along with paper plot display parameters and data storage parameters. Figure 6 shows a change in amplifier gain level on channel 1 that occured in displayed data during the cruise.

Sixteen MCS and coincident Izanagi lines were collected (Fig. 2). A data log showing reel or tape numbers, file numbers and interruptions in data collection is given in Table 4.

A one hour data gap unfortunately occurred in the critical trench and trench slope area on Line 8 when the airgun became tangled in its cable and rose to the surface. Data gaps of lengths from 5 to 15 minutes occurred as a result of a malfunction in the recording system perhaps related to overheating (cf. Table 4).

Results from Izanagi and MCS survey (Lines 1-16)

Izanagi seafloor reflectivity data plotted during data collection and is reproduced in three areas on Figures 7A, 8A, and 9A. Preliminary interpretations of these data are shown on Figures 7B, 8B, and 9B. Accompanying seismic lines with interpretations are shown in Appendix 1.

Northern area (Lines 1-6)

The northern part of this area documents diffuse seafloor faulting associated with initial trench formation (Fig. 7A). These faults are confirmed on MCS lines shown in Appendix 1, are colinear with the better developed trench to the south, and are parallel to a prominent northwest-trending gravity high seen on the Geosat map of the area. Seismic data show that the small faults exhibit both normal and reverse offsets (App. 1). Strike-slip reactivation may also be occurring. On Line 2, the zone is marked by a sag at the level of basement and the seafloor. By line 4, the same zone is marked by an arch (Appendix 1). This subtle arch will become

progressively accentuated into the trench and trench slope 40 km to the south of this locality.

We assume that this entire zone of faulting is underlain and produced by the decollement imaged on Ewing line 28 (Fig. 2). These data suggest that the zone of trench formation is occurring in a northwest direction parallel to the fracture zone fabric proposed by Winterer and Nakanishi (submitted). One hypothesis is that the decollement propagates plateauward until it intersects the preexisting fracture zone at at a depth of several kilometers. Intersection of the roughly horizontal decollement and the roughly vertical fracture zone results in reactivation of the fracture zone as a ramp or riser in the thrust system. This model may explain the rapid rise in the level of decollement seen on Ewing lines 26 and 28 (Figs. 3, 4).

This fracture zone intersection model assumes that the entire 35 km thick crust of the OJP is imprinted with a fracture zone structure as proposed by Winterer and Nakanishi (submitted). Our one long line from the 1995 Ewing survey penetrated about 125 km into the OJP and mapped complex normal and perhaps strike-slip faults formed in the flexural bulge of the OJP (Stewart arch on Figure 1). Its possible that some of these normal faults are themselves reactivated fracture zones. A key test of the fracture zone model is to run a line perpendicular to the inferred fracture zone fabric in an area unaffected by Neogene convergent tectonics (Fig. 10).

A continuous thrust front is formed in the area of line 5 and continues to the southern area mosaic (Fig. 7A). The continuous thrust front terminates on a tear fault with an orthogonal (southwest strike) and presumed strike-slip displacement. En echelon features are present on the sidescan image on the south side of the fault and are interpreted as en echelon folds and thrusts of the seafloor whose orientation is consistent with an origin by left-lateral strike-slip motion along the tear fault. In the tear fault area at line 5, the uplift is relatively symmetrical with no preferred sense of vergence. By line 6, the structure assumes a northeastward vergence which persists to the southern area of the survey.

Central area (lines 7-10)

This area shows the continued development of the main ridge as a feature bounded by a thrust on its northeastern edge (Fig. 8A). In the central area, the ridge is a narrow feature that widens markedly between

lines 10 and 11. Nakanishi and Winterer (this report) have noted that the ridge from line 10 to the south is marked by a linear magnetic anomaly. This anomaly may reflect uplift of a greater volume of basement material along this wider and higher part of the ridge south of line 10. No trench fill is present along the ridge in the central area because the bathymetric trench remains small and does not form a depocenter.

Lines 6-9 show anomalous, regularly spaced highs in the pelagic section within the forming trench. These highs appear to be anticlines above blind thrusts which are propagating seaward from the main thrust. On line 10, these inferred trench faults appear to reverse their motion as down-to-the-trench normal faults, perhaps related to plate bending of the Ontong Java Plateau.

On lines 11 through 16, these faults are not visible perhaps because of a thicker trench fill that overlies the incoming pelagic section. Shortening on these lines appears to be accommodated by small folds at surficial levels within the trench fill section. These small folds are expressed on the seafloor by a corrugated-like surface which exhibits a trench-parallel strike on the sidescan image, particularly near lines 13, 14, and 15 (Fig. 8B).

The increase in ridge elevation at line 10 is also accompanied by the formation of a deeper trench and trench slope basin landward of the ridge. This basins are depocenters for higher reflectivity reworked sediments derived from one of the following sources: 1) highs along the Stewart arch of the Ontong Java Plateau (including Ontong Java atoll); 2) erosion of the scarp itself; and 3) erosion of the Solomon Islands. A fold-related borderland topography of the Malaita prism prevent much of the Solomon Island terrigenous material from reaching the trench (Fig. 1). A possible canyon system linking the Ontong Java atoll with the trench is traced on the bathymetric map shown in Figure 2.

The seaward, feather edge of the trench fill is marked by a faint lineament on sidescan imagery. This feather edge appears to be locally controlled by cuesta-like features on the upper surface of the pelagic section such as on lines 14, 15, and 16.

Southern area (lines 12-16)

The southern area is characterized by a complex junction of two

arcuate parts of the main thrust of the North Solomon trench (Fig. 9A). The northern arcuate segment is seen on lines 5-14 and a southern arcuate segment is seen on lines 14-16. This cusp marks the join between the Choiseul and Santa Isabel structural domains of Phinney (1997) (Fig. 1). The cusp area of the OJP is marked by a gravity low which is attributed to an increased thrust load imparted by the two overriding plates.

The widening and thickening trench fill seen on Lines 14-16 occupies this gravity low. A feature prominent on lines 13-16 in the southern area, which are not observed to the north, are long, straight channels extending down the slope of the Stewart arch into the North Solomon trench (Fig. 9A). Seismic lines 14-16, which cross the features at a high angle, reveal these features to be channels incised in the upper surface of the pelagic carbonate unit. These features can be traced as faint lineaments that extend into the trench fill unit. This relationship suggests that the channels may be important funnels for shallow water sediment from the Stewart arch that fills the trench from the northeast. The channel area of lines 14-16 is on the trend of a bathymetric canyon visible on the bathymetric map in Figure 2. This canyon system bifurcates near a large seamount on the flank of the Steward arch. The northern branch of the system appears on trend with Ontong Java atoll.

It appears that the younger Choiseul structural domain may overthrust the older and longer lived Santa Isabel domain in the vicinity of line 14 as shown by Phinney (1997) (Fig. 1). However, the nature of this contact is not clear on the sidescan image.

The low between the frontal ridge and main scarp on lines 15 and 16 is starved of trench fill. This would suggest that the main scarp is not a major source of trench fill sediments which would instead be derived from either the Stewart arch to the northeast or the Solomon Islands to the southwest.

A characteristic feature of the Santa Isabel domain on lines 14-16 is a frontal ridge composed of accreted OJP basalt and pelagic limestone (Appendix 1). This frontal ridge formed by frontal accretion of the incoming OJP section attests to longer lived subduction along the Santa Isabel structural domain. The frontal ridge is propagating northward into the Choiseul structural domain because a nascent ridge can be seen on lines 13 and 14.

Significance of this study

The cross sectional MCS data can be viewed as a time series for the evolution of the North Solomon trench. While subduction at this site has been longlived with a prior Tertiary subduction history along the KKK fault zone in the Solomon Islands (Fig. 1), these data reveal the seaward propagation of this zone as a result of subduction of 35-km-thick OJP crust. Figure 10 shows a map of inferred fracture zones in the area from Winterer and Nakanishi (submitted) that may act as potential pathways for the seaward propagation of the evolving subduction zone. If this model is correct, the spacing between fracture zones on the OJP will be the width of blocks of oceanic plateau that are added to the front of the Malaita accretionary prism. It is interesting to note on Figure 10 that the width of the Malaita accretionary prism is approximately the same width as the areas of oceanic plateau crust isolated by fracture zones to the northeast.

Future work

Some possible followup surveys include the following:

· **Confirmation of fracture zone structures along gravity highs and lows seen on Geosat gravity map in the incoming, undeformed part of the OJP.** Inspection of bathymetric and gravity maps for the OJP in the Solomon-Bougainville-New Ireland area reveals a prominent linear trend which may be a continuous fracture zone now entering the trench. The prominence of this trend suggests that it may be undergoing reactivation perhaps as the new frontal thrust of this suduction zone.

· **Shallow piston core drilling of slope basins and trench sediments to determine the rate at which the new subduction zone is forming.** Piston coring combined with biostratigraphy of the trench fill and two upper slope basins would provide high resolution rate information on the process of subduction initiation. Rich late Neogene microfauna could provide age resolution to the 100 Ka time frame. Age information could also be used to confirm the rates of tilting and shortening that can be determined using existing seismic data. Comparable studies have been proposed for slope basins in the Makran area but high terrigenous sedimentation rates "drown

out" microfauna making dating difficult.

· **Hard rock drilling of the thrust contact within the OJP.** There are few if any examples known of basalt to basalt thrust contacts along active faults in a marine setting. Most thrusts investigated by ODP involve sediment-sediment contacts in traditional accretionary prism settings. The investigation of this contact could lead to advances in understanding the mechanics and seismicity of hard rock thrust contacts that are normally found at depths too great for drilling.

References

Phinney, E., 1997, Sequence stratigraphy, structure, and tectonics of the southern Ontong Java Plateau and Malaita accretionary prism, Solomon Islands, unpublished MA thesis, University of Texas at Austin, 128 p.

Winterer, E. L., and Nakanishi, M., Evidence for a plume-augmented, abandoned, Early Cretaceous spreading center on Ontong Java Plateau, manuscript submitted to JGR, January, 1998.

Figure captions

Figure 1. Tectonic setting of the North Solomon trench, Malaita accretionary prism (MAP), and Solomon island arc (from Phinney, 1997). Box indicates location of more detailed map in Figure 2. The Malaita accretionary prism consists of accreted fragments of the Ontong Java Plateau that is subducting to the southwest beneath the prism and Solomon island arc. The prism is divided into four structural domains based on the arcuate shape of the North Solomon trench the trends of the numbered anticlinal axial traces within each domain. Dashed lines are interpreted from linear gravity trends. Dark gray shading adjacent to to the domain boundaries indicates large-amplitude free-air gravity lows associated with foredeeps adjacent to the prism. Light gray shading within the MAP indicates negative free-air gravity anomalies associated with bathymetric lows and depositional basins. Key to abbreviations: BG = Bougainville; CH = Choiseul; G = Guadalcanal; INB = Indispensable basin; KKKF = Kia-Kaipito-

Korigole fault zone; KT = Kilinailau trench; M = Malaita; MK = Makira; N = Ndai; NBT = New Britain trench; NG = New Georgia Island Group; NST = North Solomon trench; R = Ramos; SH = Shortland Islands; SI = Santa Isabel; ST = Simbo transform fault; U = Ulawa; WSR = Woodlark spreading ridge.

Figure 2. Map of ship tracks and data collected during North Solomon trench survey. MCS lines 19 through 32 were collected in 1995 by the RV Maurice Ewing. Initial KH-98 lines were transit lines to deploy OBS instruments NC1, NC2, and NC3. MCS and Izangi data commenced on Line 1 and continued through Line 16. Heavy line denotes Seabeam line run through the area to better constrain the Izanagi bathymetry. Line to northeast of North Solomon trench indicates possible submarine canyon system that could provide highly reflective trench fill of North Solomon trench seen in the southern part of the study area.

Figure 3. Decollement imaged on 1995 Ewing MCS line underlying accreted section of the OJP at the Choiseul structural domain (from Phinney, 1997). Note fold in seafloor in the area where the decollement cuts up section through the Cretaceous basement of the OJP. The decollement dips southwest at 10 degrees and penetrates to a depth greater than 6.7 km below the seafloor. Three OBS instruments were deployed on the seafloor in a triangle above this area to record possible microseismicity associated with this fault (cf. Figure 2).

Figure 4. Decollement imaged on 1995 Ewing MCS line underlying accreted section of the OJP at the Choiseul structural domain (from Phinney, 1997). The fault dips southwest at 17 degrees and penetrates to a depth greater than 7 km beneath the seafloor. Increasing relief at the anticline above this feature suggests that fault offset increases in a southeasterly direction.

Figure 5A. Schematic map showing Izanagi towing configuration used during KH-98-1 survey. B. Schematic cross section showing how Izanagi acoustic arrival angles are measured.

Figure 6. Change in amplifier gain level on channel 1 that occured in

displayed data during the cruise.

Figure 7A. Sidescan mosaic of northern area. B. Interpretation by A. Taira.

Figure 8A. Sidescan mosaic of northern area. B. Interpretation by P. Mann.

Figure 9A. Sidescan mosaic of northern area. B. Interpretation by P. Mann

Figure 10. Inferred fracture zone structure of the OJP by Winterer and Nakanishi (submitted).

Table 1. Acquisition parameters for KH-98-1 MCS seismic system.

Table 2. Parameters o KH-98-1 streamer, plotting of singl e trace record, and data storage.

Table 3. MCS data log for KH-98-1 showing reel numbers, start and ends of lines, and data interruptions. The recording system did not record shot numbers.

Appendix 1. Seismic lines 1-16 for the North Solomon trench (single trace monitor record). Stratigraphic interpretations by J. Winterer, structural interpretations by A. Taira with minor modifications by P. Mann.

original figures

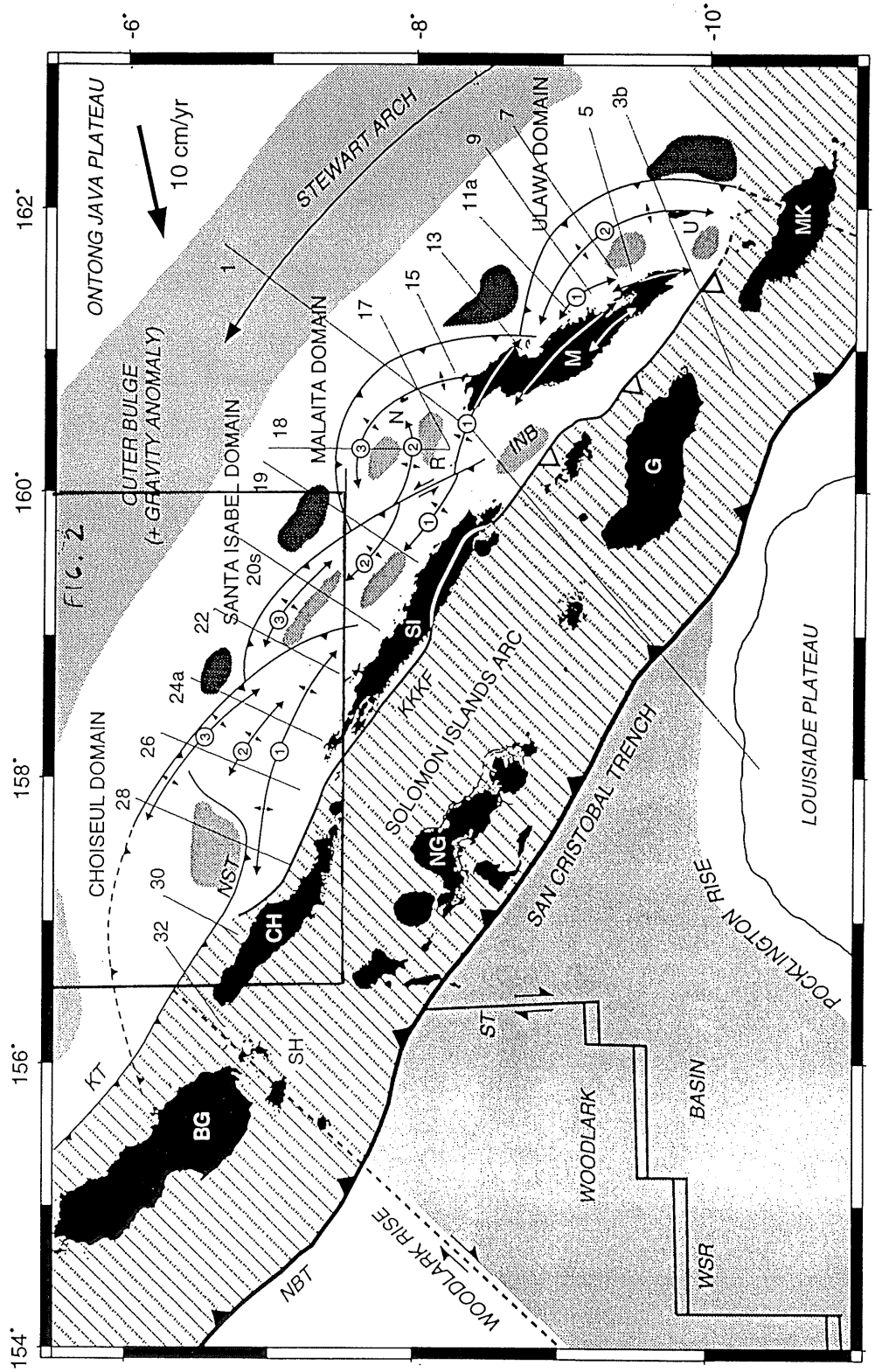

(FIG. 1)

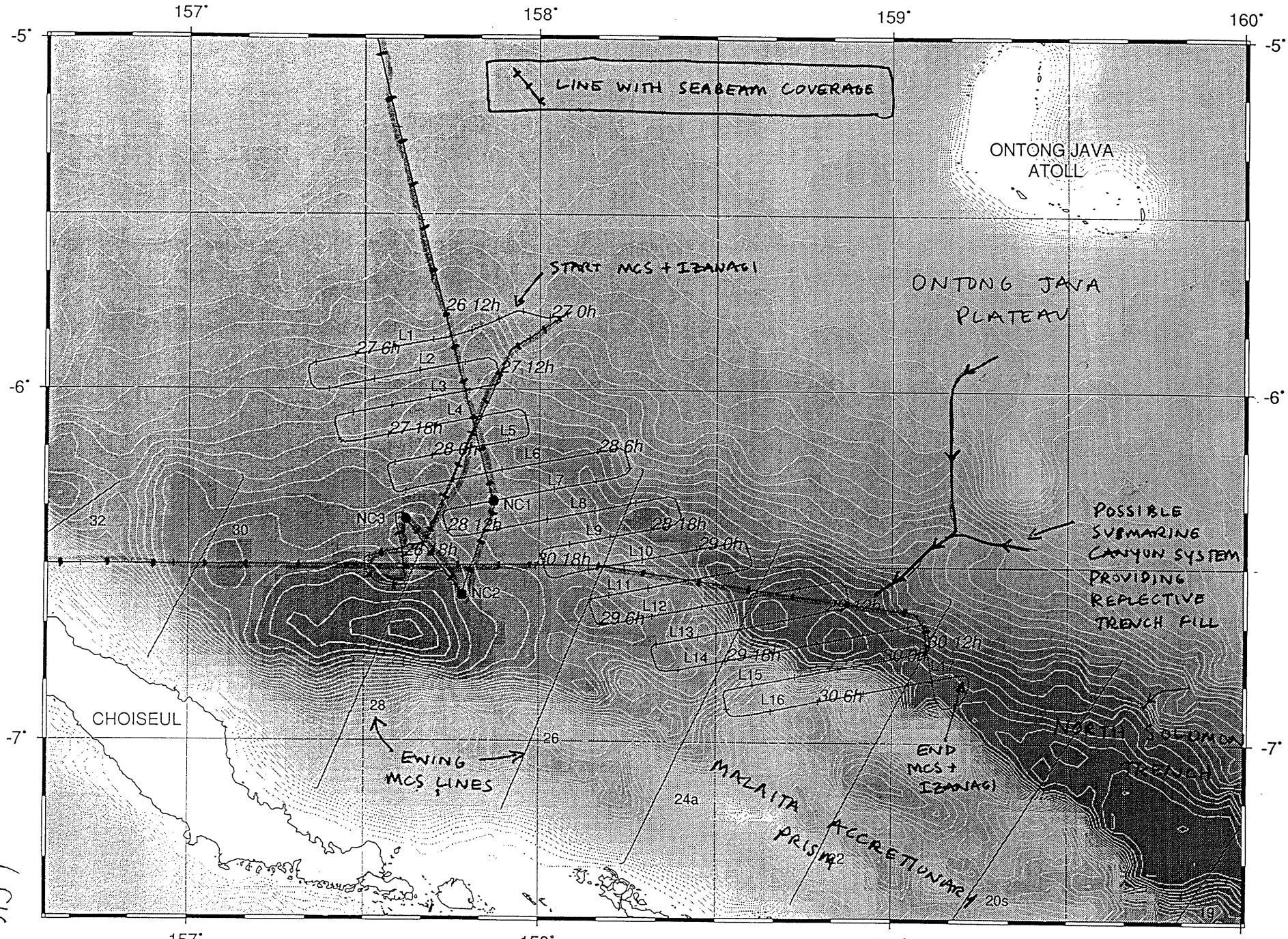
157°
158°
159°
160°
-5°
-6°
-7°
LINE WITH SEABEAM COVERAGE
ONTONG JAVA ATOLL
START MCS + IZANAGI
ONTONG JAVA PLATEAU
26 12h
27 0h
27 6h
27 12h
27 18h
28 0h
28 6h
28 12h
28 18h
29 0h
29 6h
30 0h
30 12h
30 18h
L1
L2
L3
L4
L5
L6
L7
L8
L9
L10
L11
L12
L13
L14
L15
L16
NC1
NC2
NC3
32
30
28
26
24a
20s
19
POSSIBLE SUBMARINE CANYON SYSTEM PROVIDING REFLECTIVE TRENCH FILL
CHOISEUL
EWING MCS LINES
END MCS + IZANAGI
MAZAITA ACCRETIONARY PRISM
NORTH SOLOMON TRENCH

FIG-2

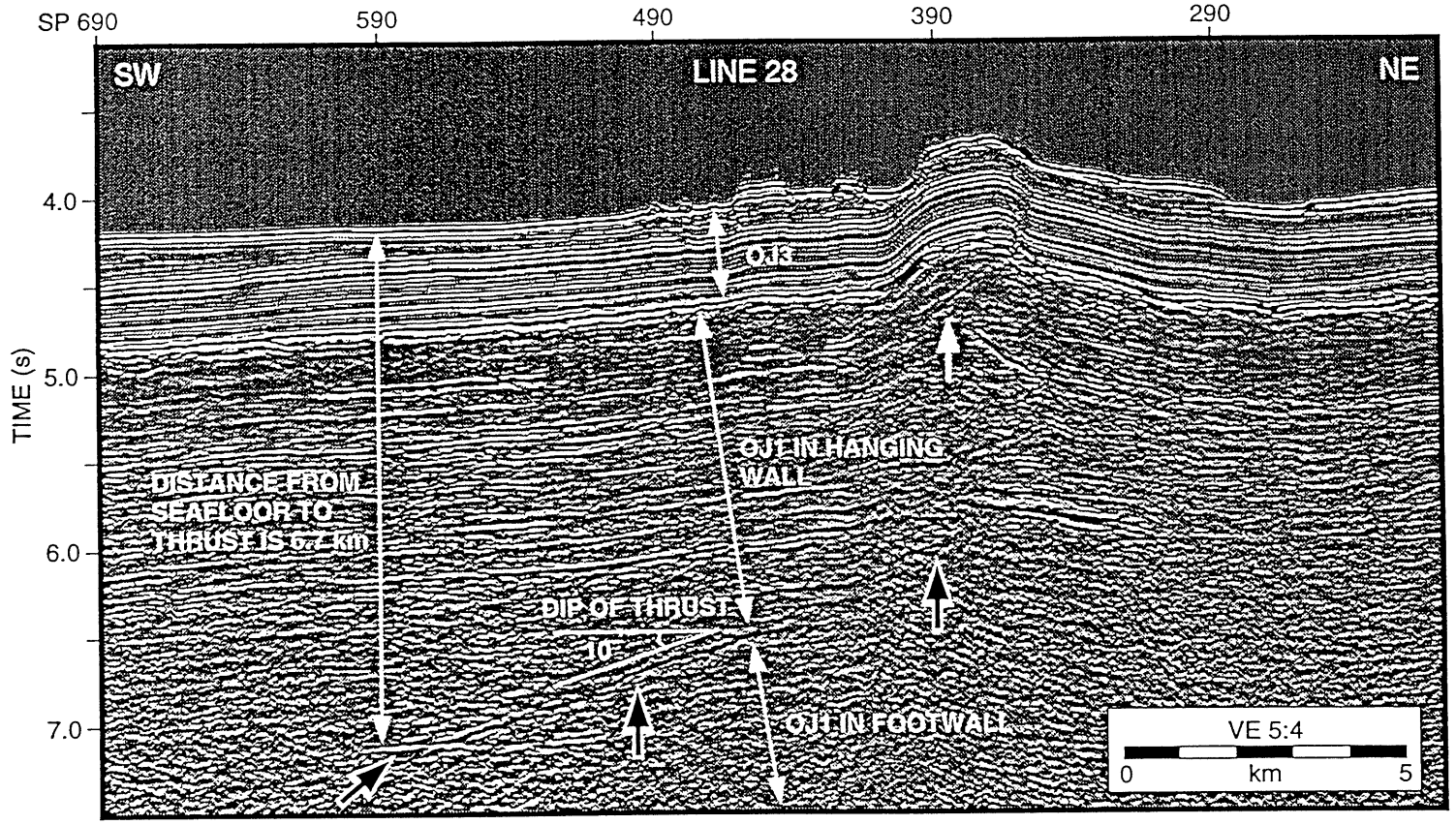

~~Figure 3.9~~. Main thrust underlying accreted section of OJP constituting the Choiseul structural domain as imaged on Line 28. The fault dips southwest at 10° and penetrates a depth greater than 6.7 kmbsf southwest of SP 590. Short-wavelength seafloor deformation is caused by smaller faults (white arrow) branching off of main thrust (black arrow). See Figure 3.6 for location.

(Fig. 3)

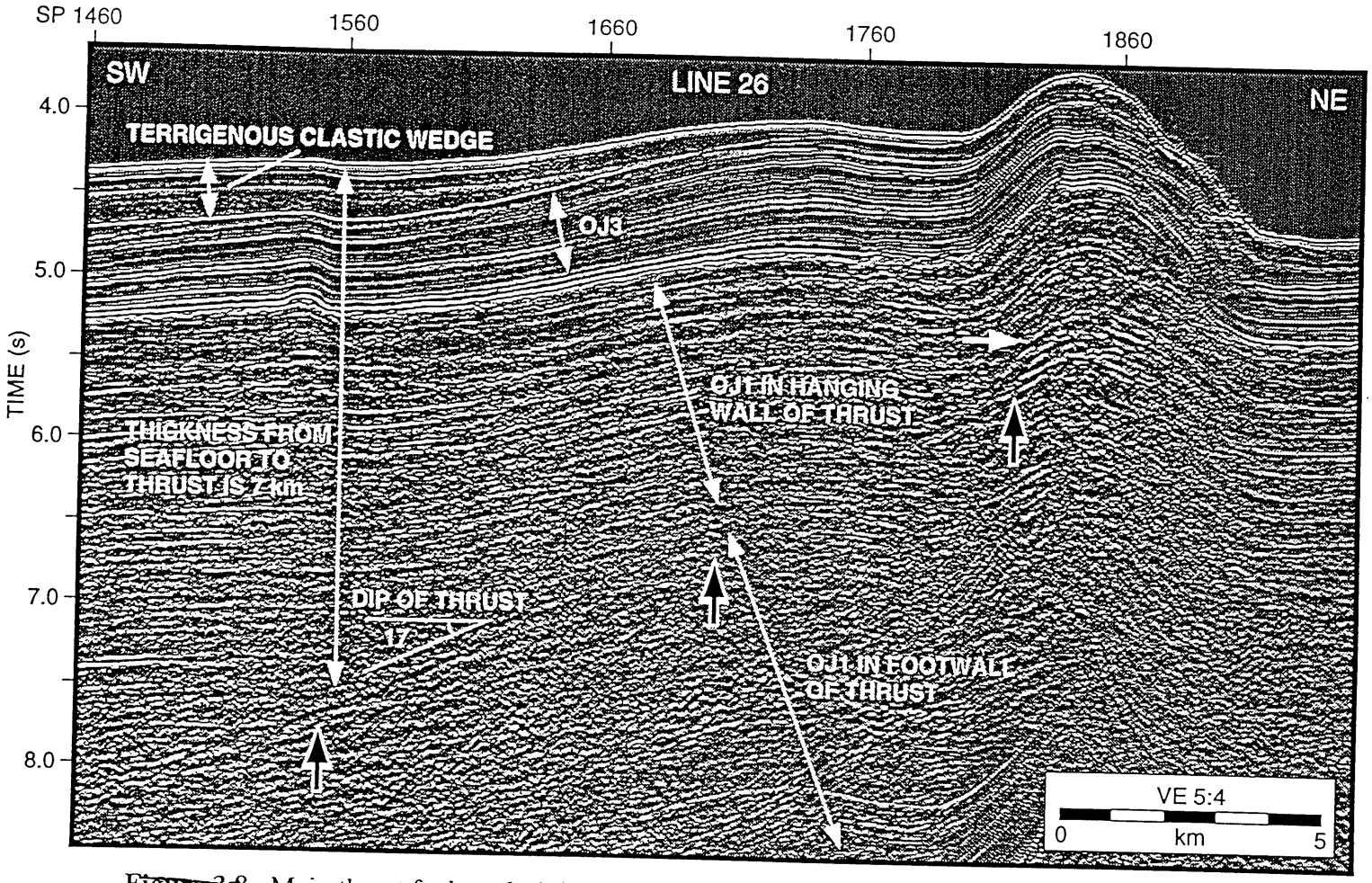

~~Figure 3.8~~. Main thrust fault underlying accreted section of OJP constituting Choiseul structural domain as imaged on Line 26. The fault dips southwest at 17° and penetrates a depth greater than 7 kmbsf southwest of SP 1560. Short-wavelength seafloor deformation is caused by smaller faults (white arrow) branching off main thrust (black arrows).

(Fig. 4)

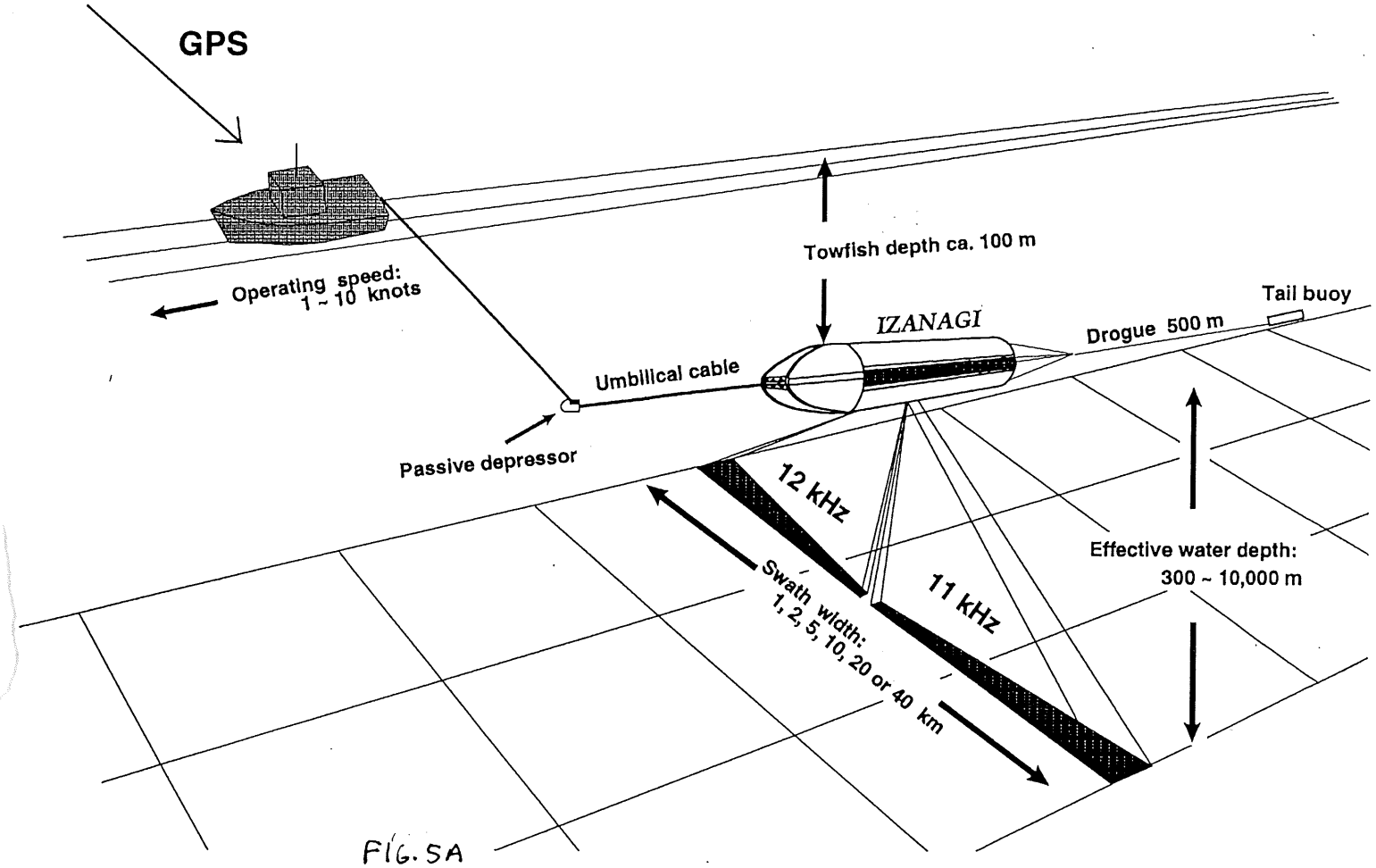

FIG. 5A

~~Fig. 1~~ *IZANAGI* Towing configuration schematic

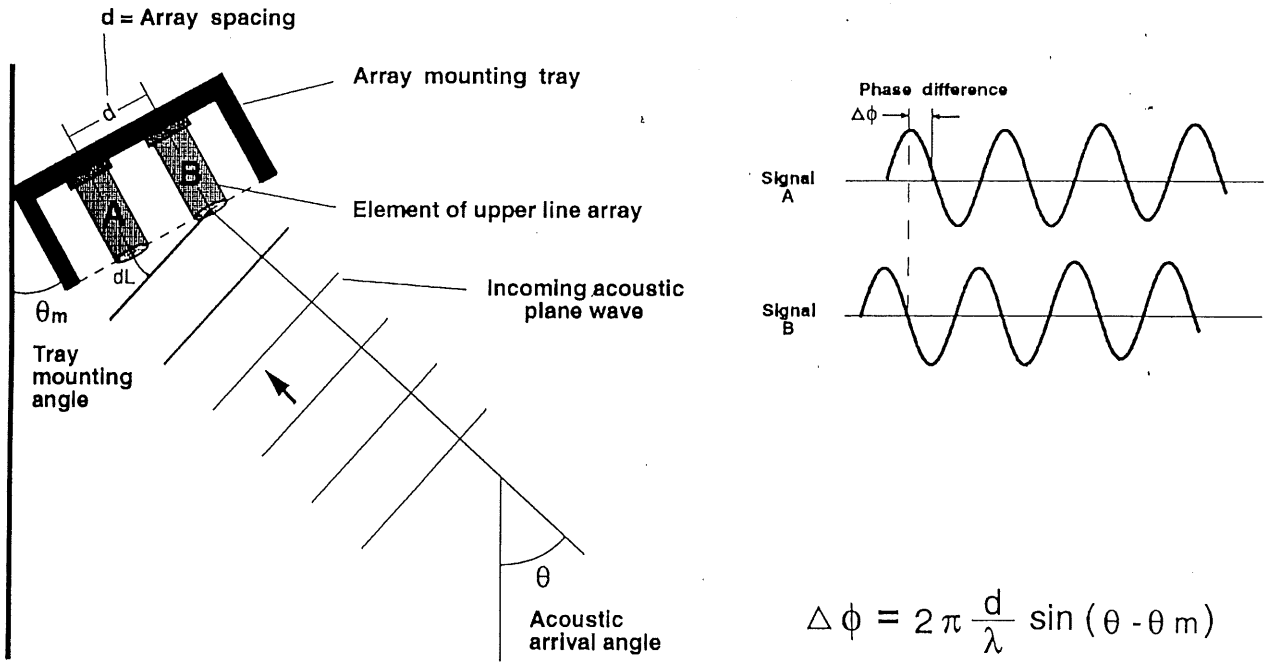

FIG. 5B

~~Fig. 2~~ Acoustic arrival angle measuring geometry

(Fig 5A, 5B

KH-98-1 MCS system

~~1/3~~ 1/27 05:34:00

ch1 48dB

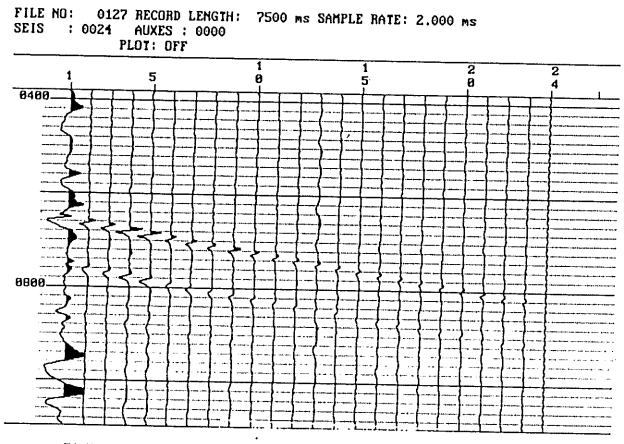

Channel 1
48 dB

1/30 05:31:00

ch1 24dB

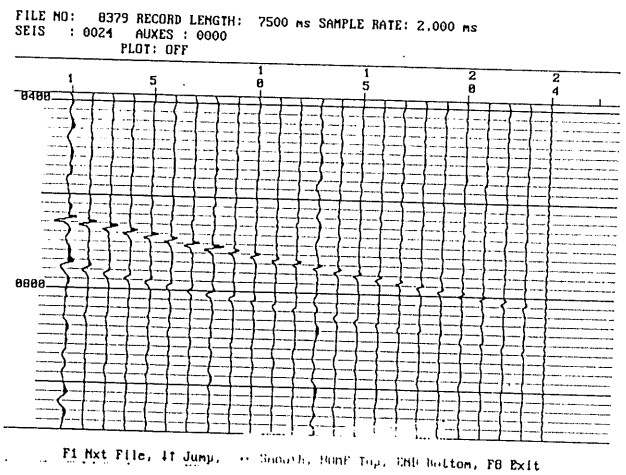

Channel 2
24 dB

(Fig. 6)

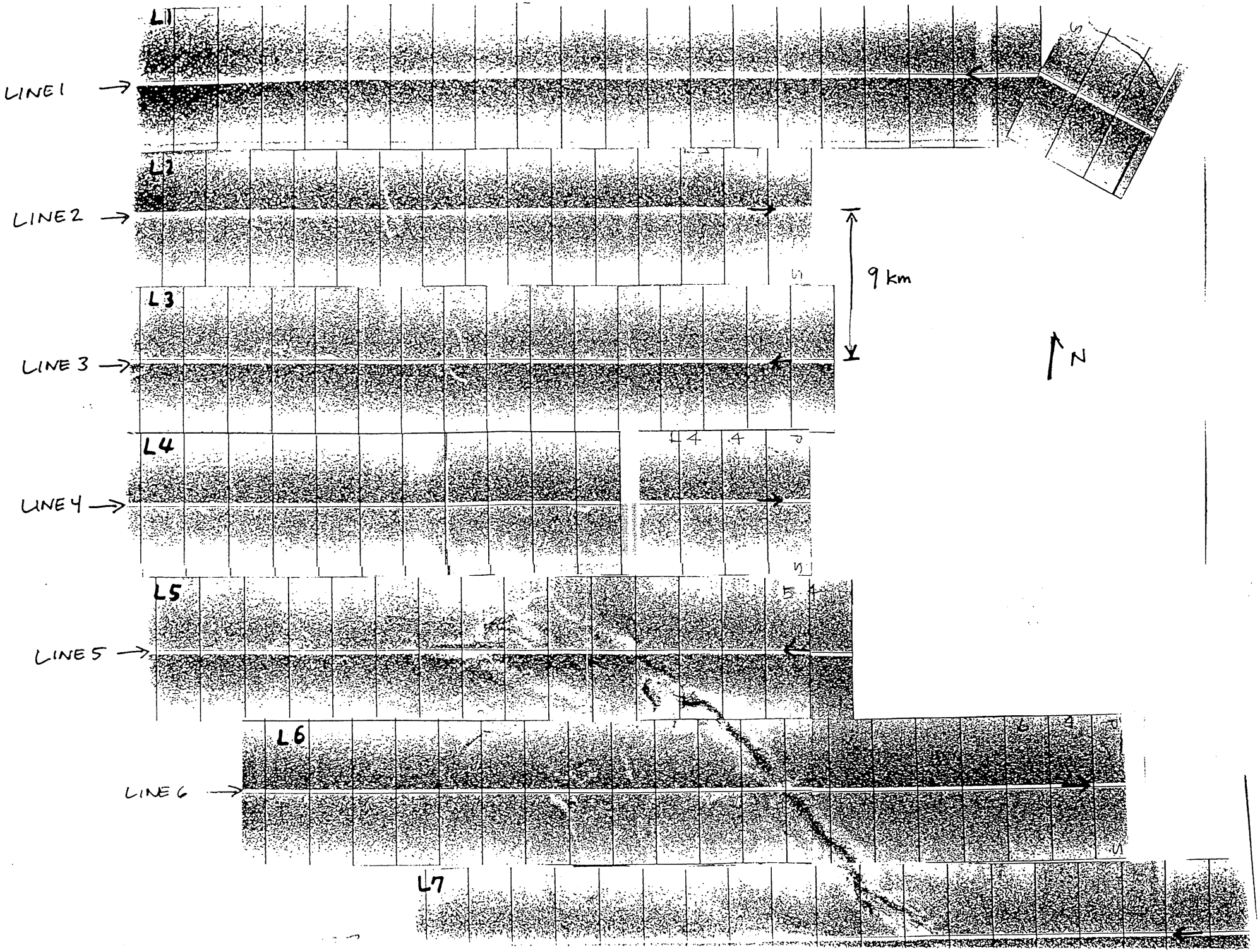

(Fig. 7A - Northern Area mosaic)

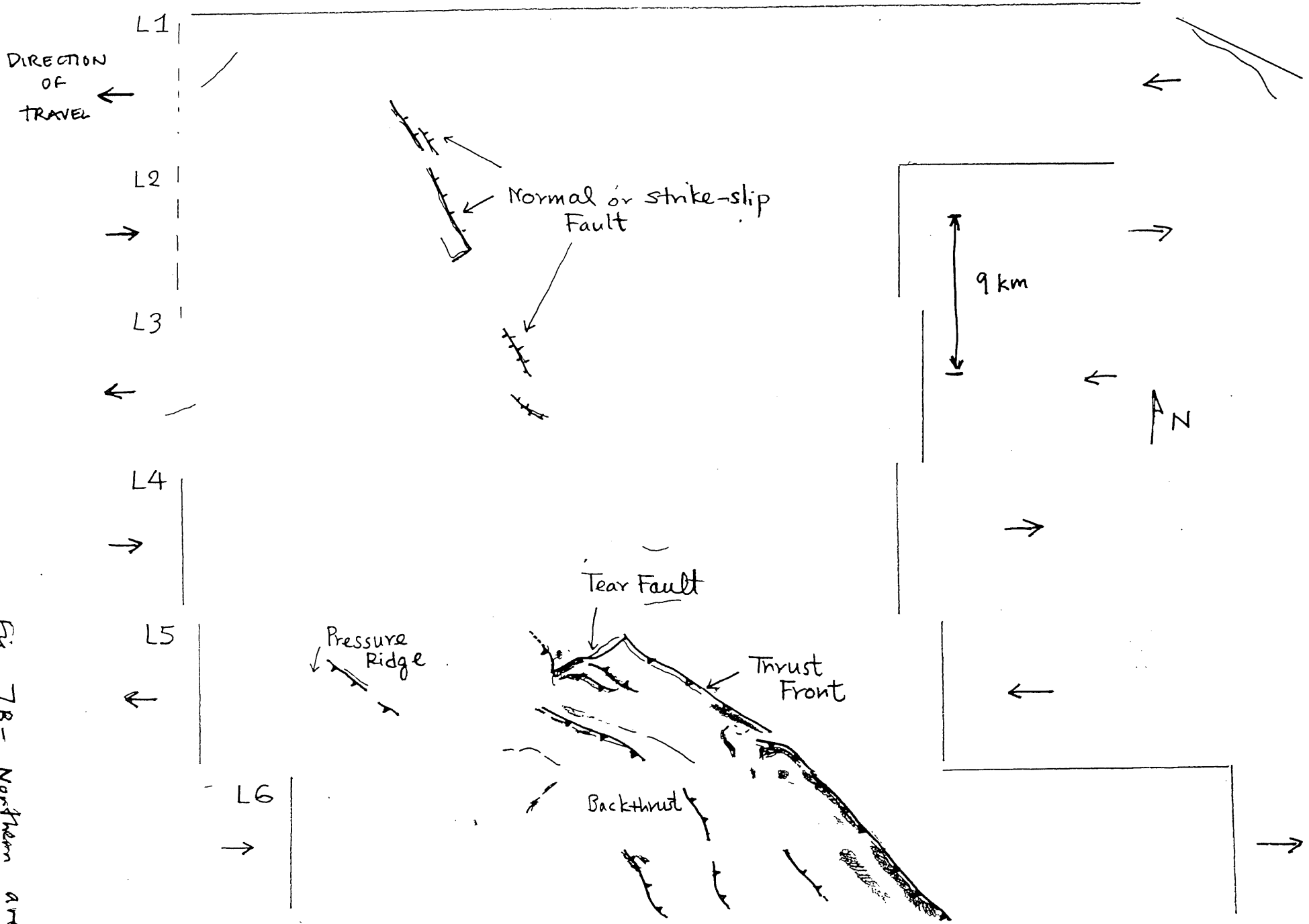

Fig 7B - Northern area interpretation by A. Tavia

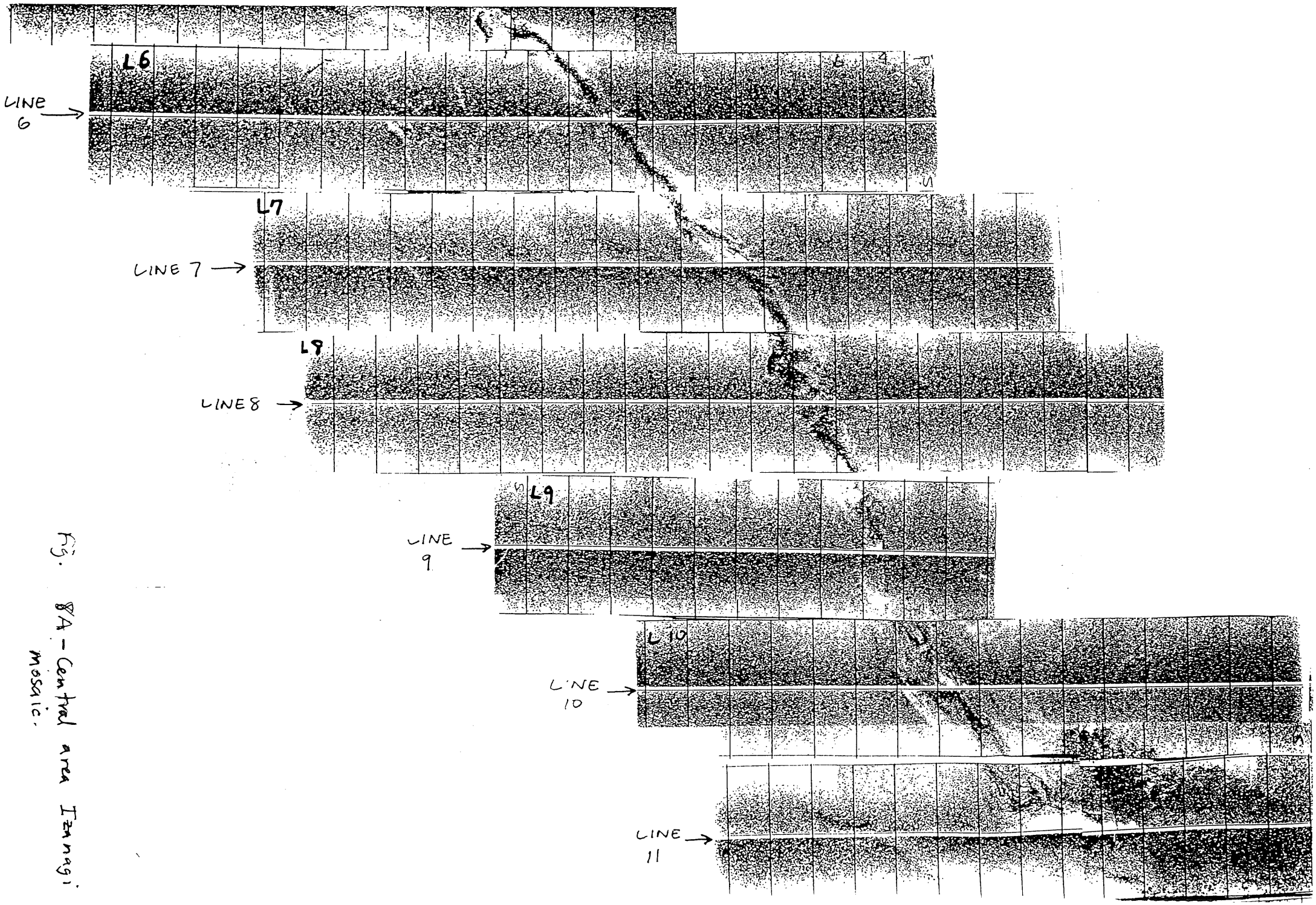

Fig. 8A - Central area Izunagi mosaic.

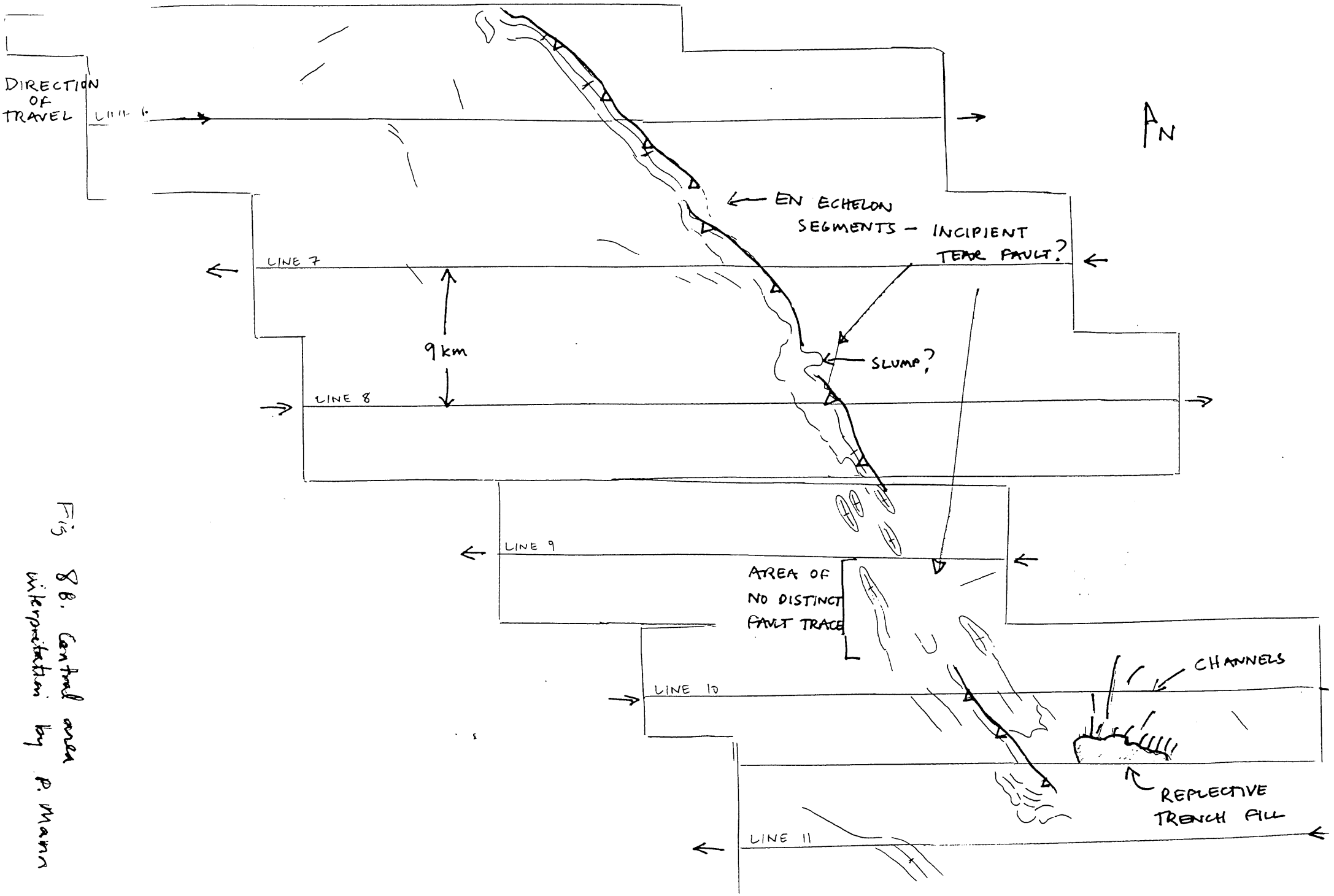

Fig 8B. Central area interpretation by P. Mann

Fig 9A. Southern area Izanagi mosaic.

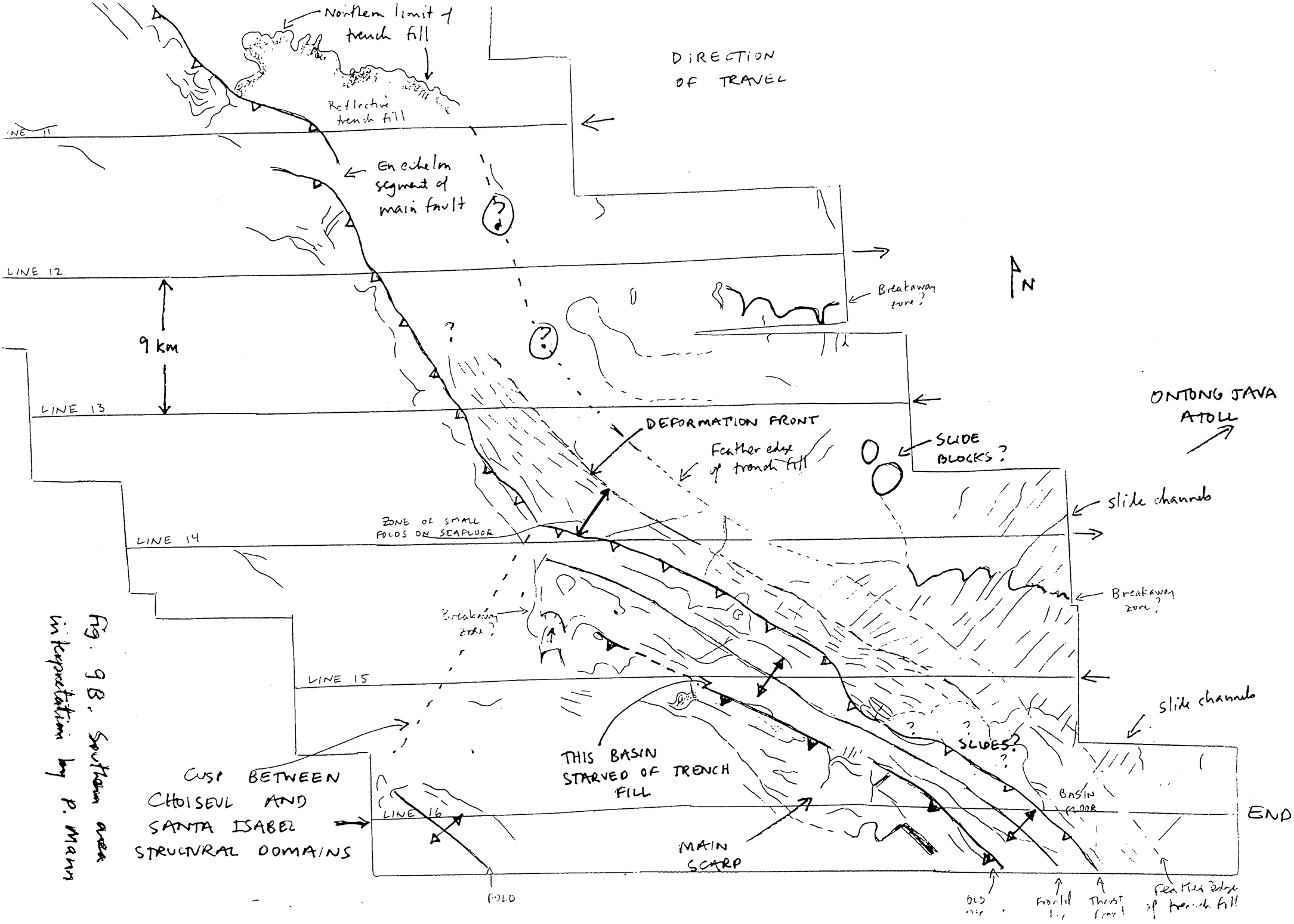

Fig. 9B. Southern area interpretation by P. Mann

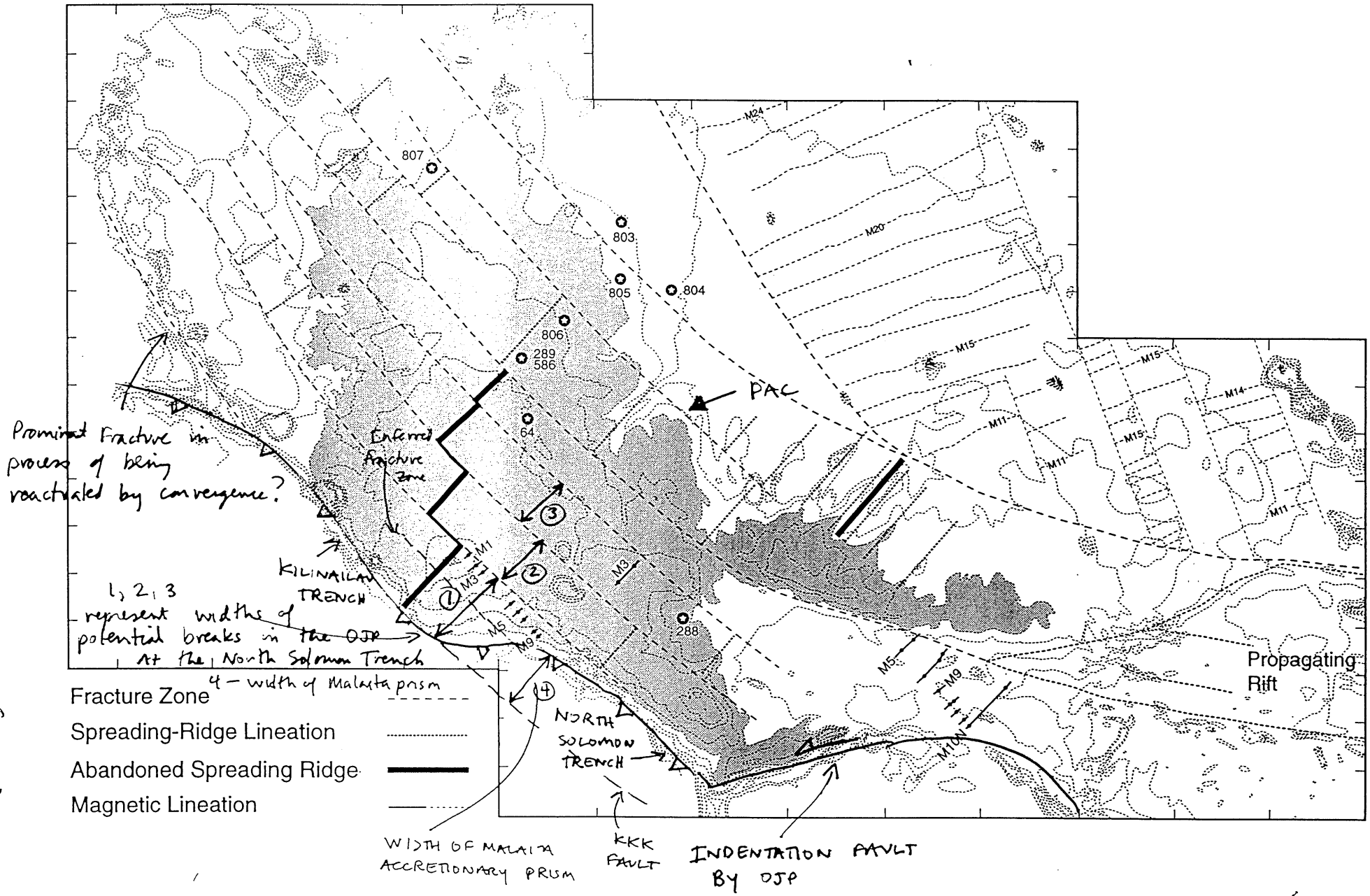

(Fig. 10)

Winterer & Nakanishi, Fig. 7 (submitted, 1998)

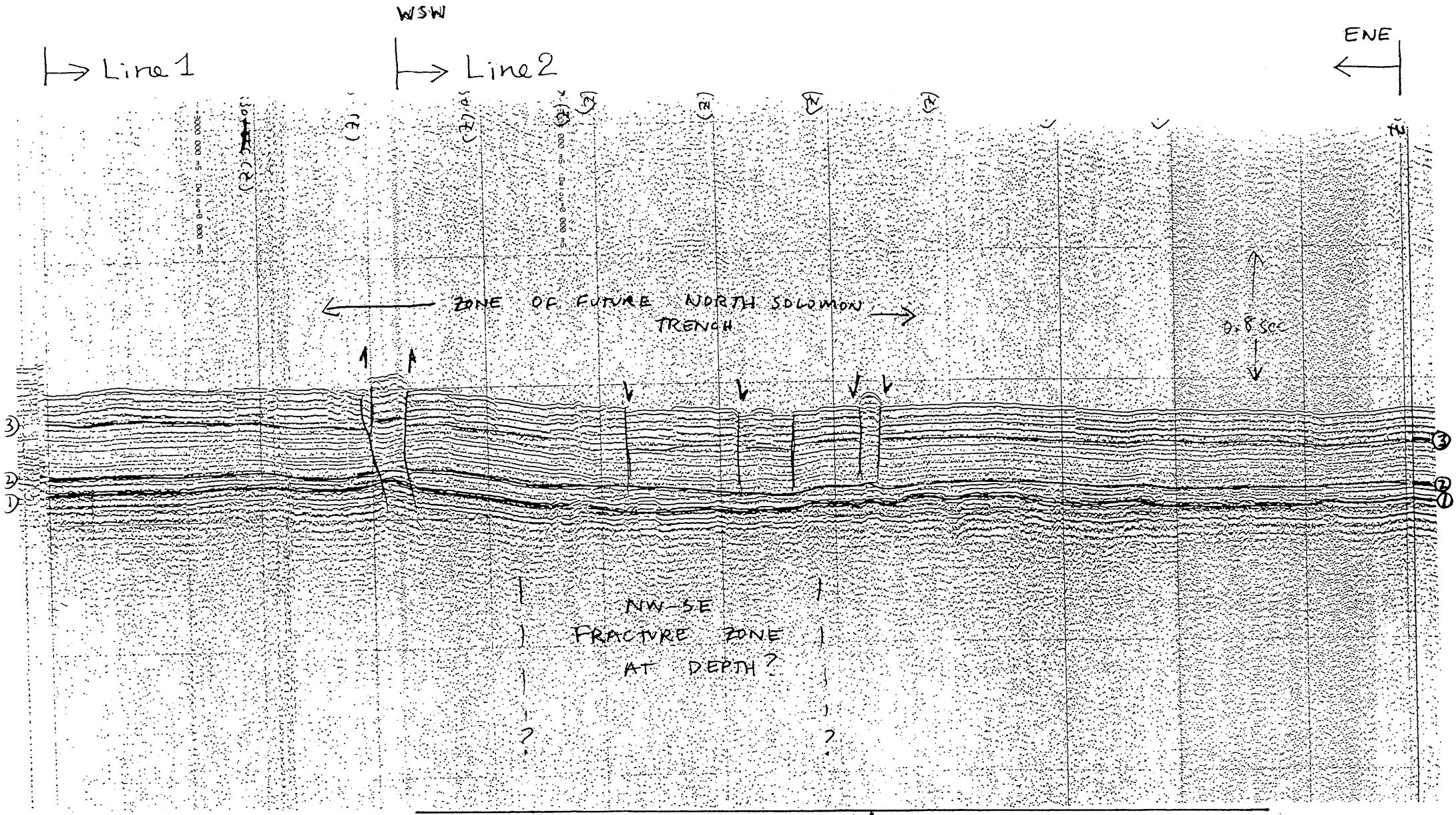

KEY TO NUMBERED REFLECTORS:

1 = TOP ONTONG JAVA PLATEAU BASALTIC BASEMENT (CRETACEOUS)

2 = TOP CHERT (EOCENE)

3 = PROMINENT REFLECTORS (TRIPLET) WITHIN EOCENE - RECENT PELAGIC SECTION

PICKS BY JERRY WINTERER

(App. 1)

ESE

→ Line 3

WNW

←

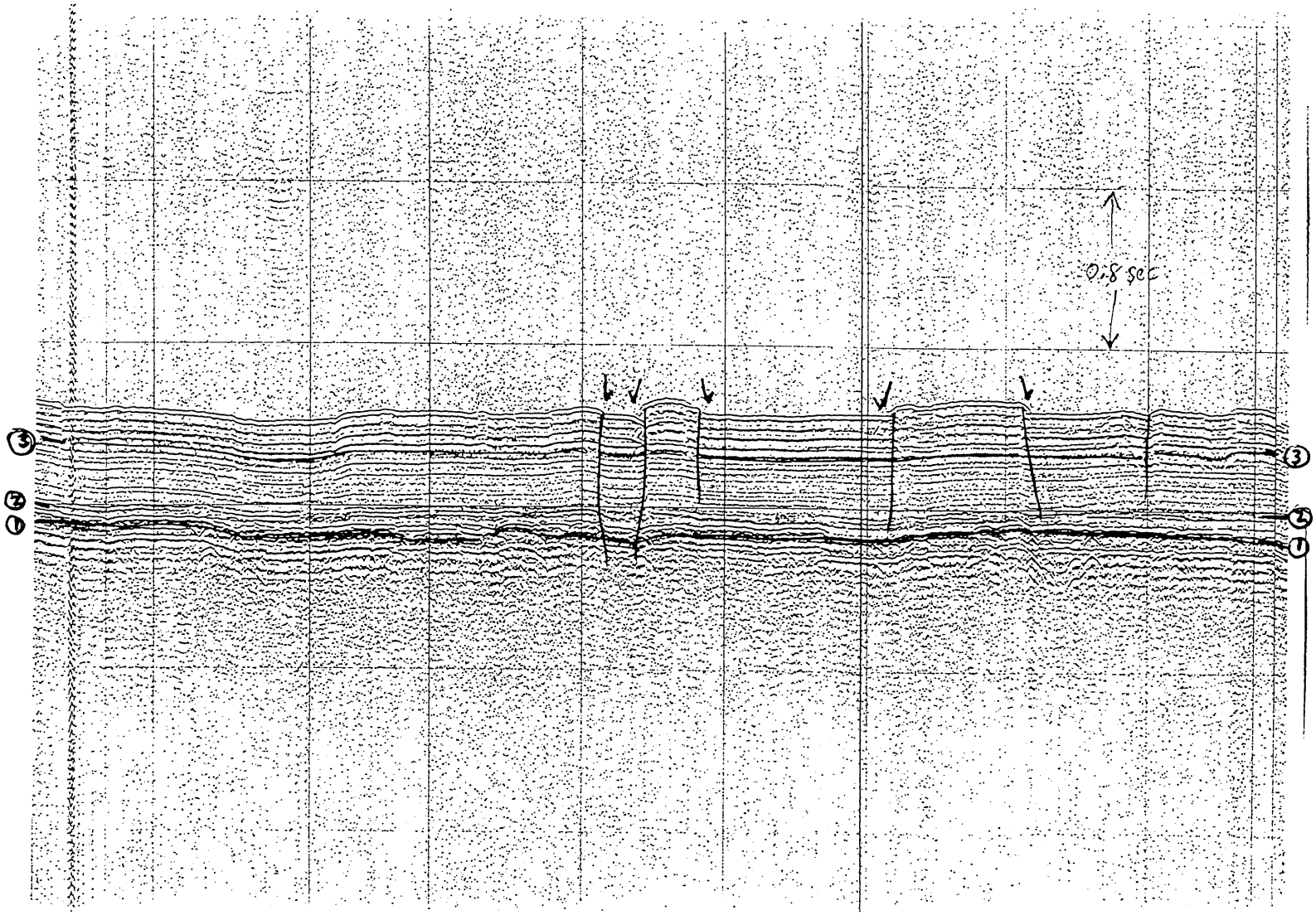

LINE 3

LINE 4

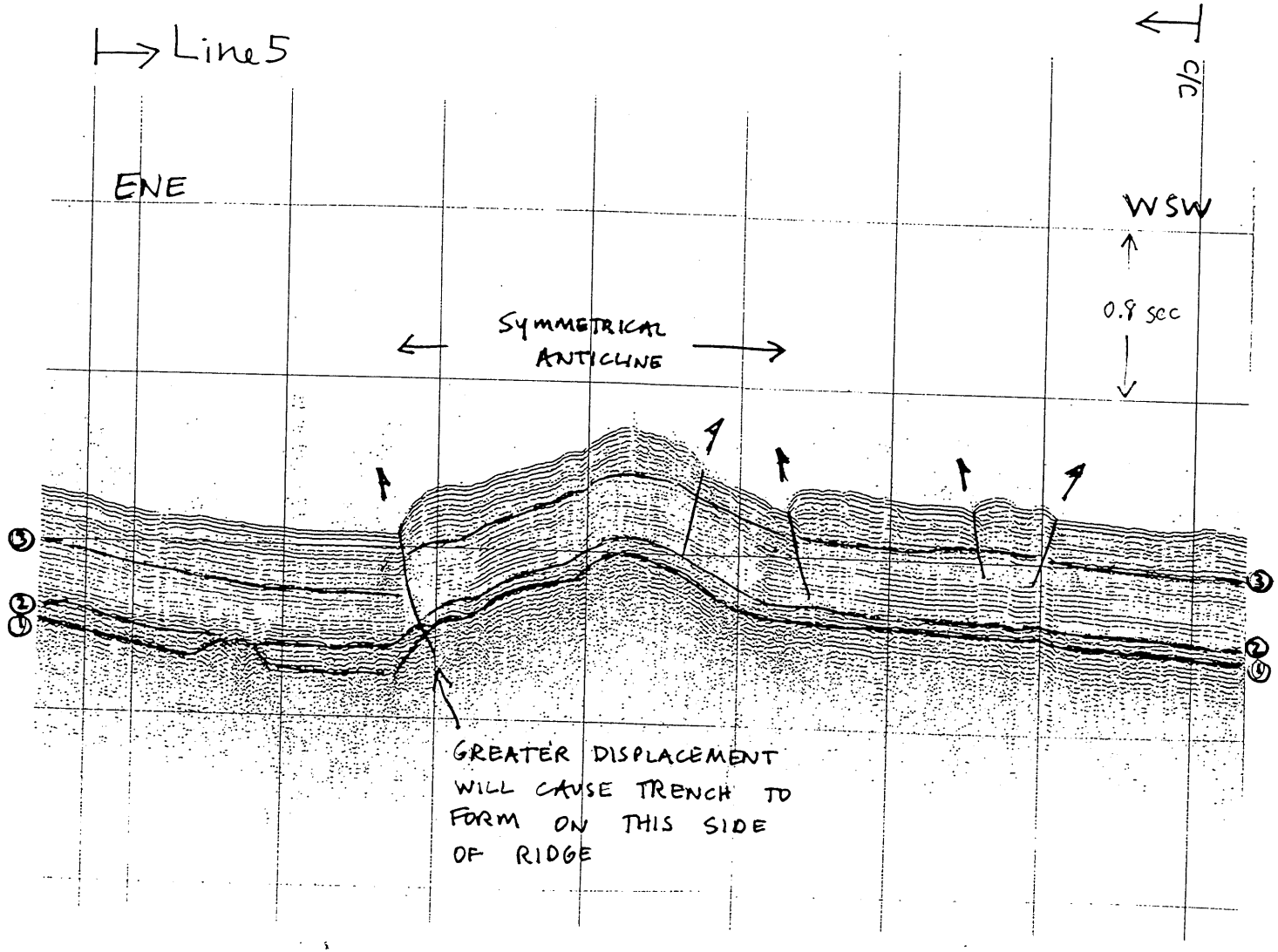
Line 5
C/C
ENE
WSW
0.8 sec
SYMMETRICAL ANTICLINE
3
2
1
GREATER DISPLACEMENT WILL CAUSE TRENCH TO FORM ON THIS SIDE OF RIDGE

LINE 5

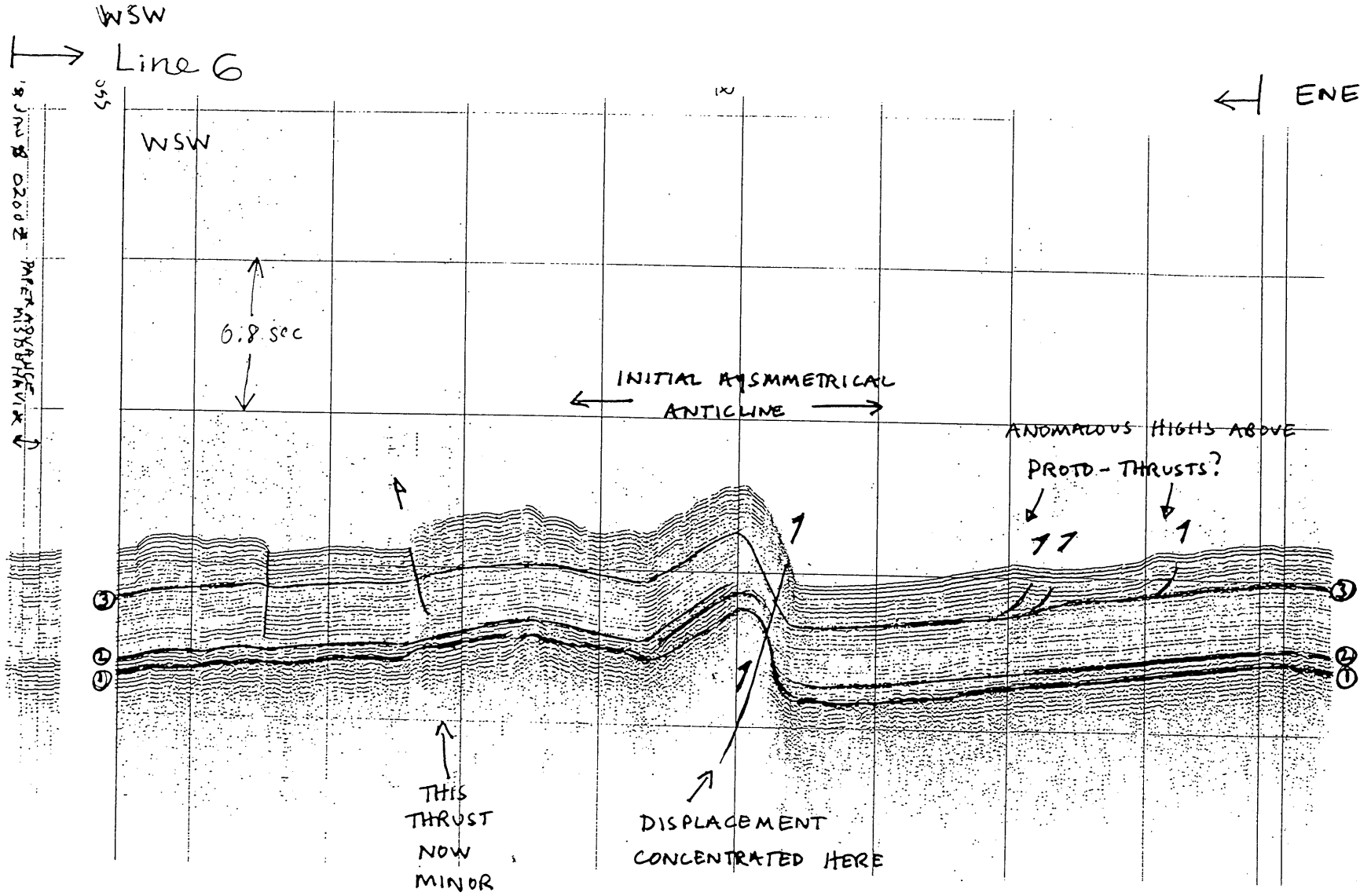
WSW
Line 6
ENE
WSW
6.8 sec
INITIAL ASYMMETRICAL ANTICLINE
ANOMALOUS HIGHS ABOVE PROTO-THRUSTS?
THIS THRUST NOW MINOR
DISPLACEMENT CONCENTRATED HERE
3
2
1

LINE 6

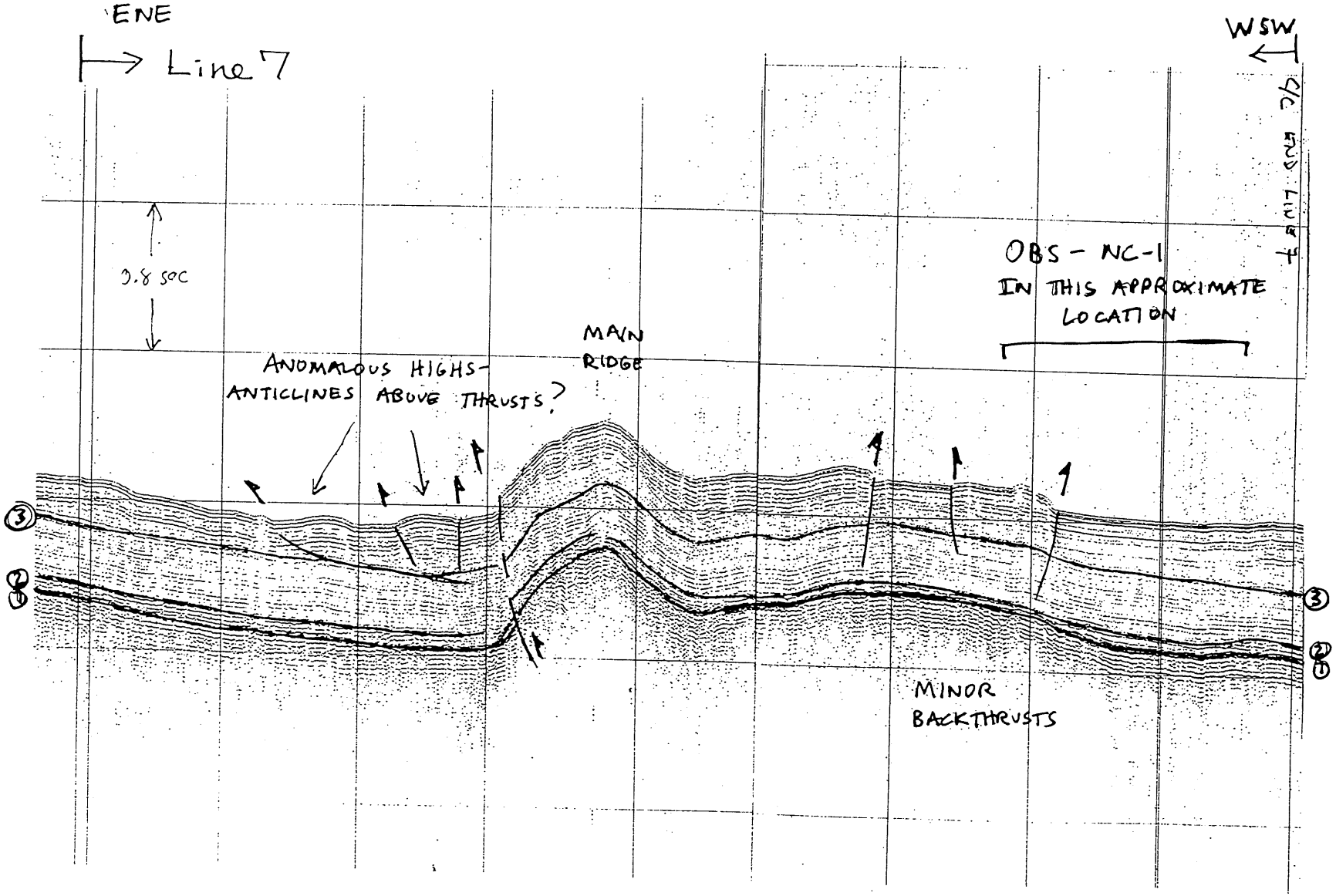
ENE
Line 7
WSW
0.8 sec
OBS - NC-1
IN THIS APPROXIMATE
LOCATION
MAIN
RIDGE
ANOMALOUS HIGHS-
ANTICLINES ABOVE THRUSTS?
MINOR
BACKTHRUSTS

LINE 7

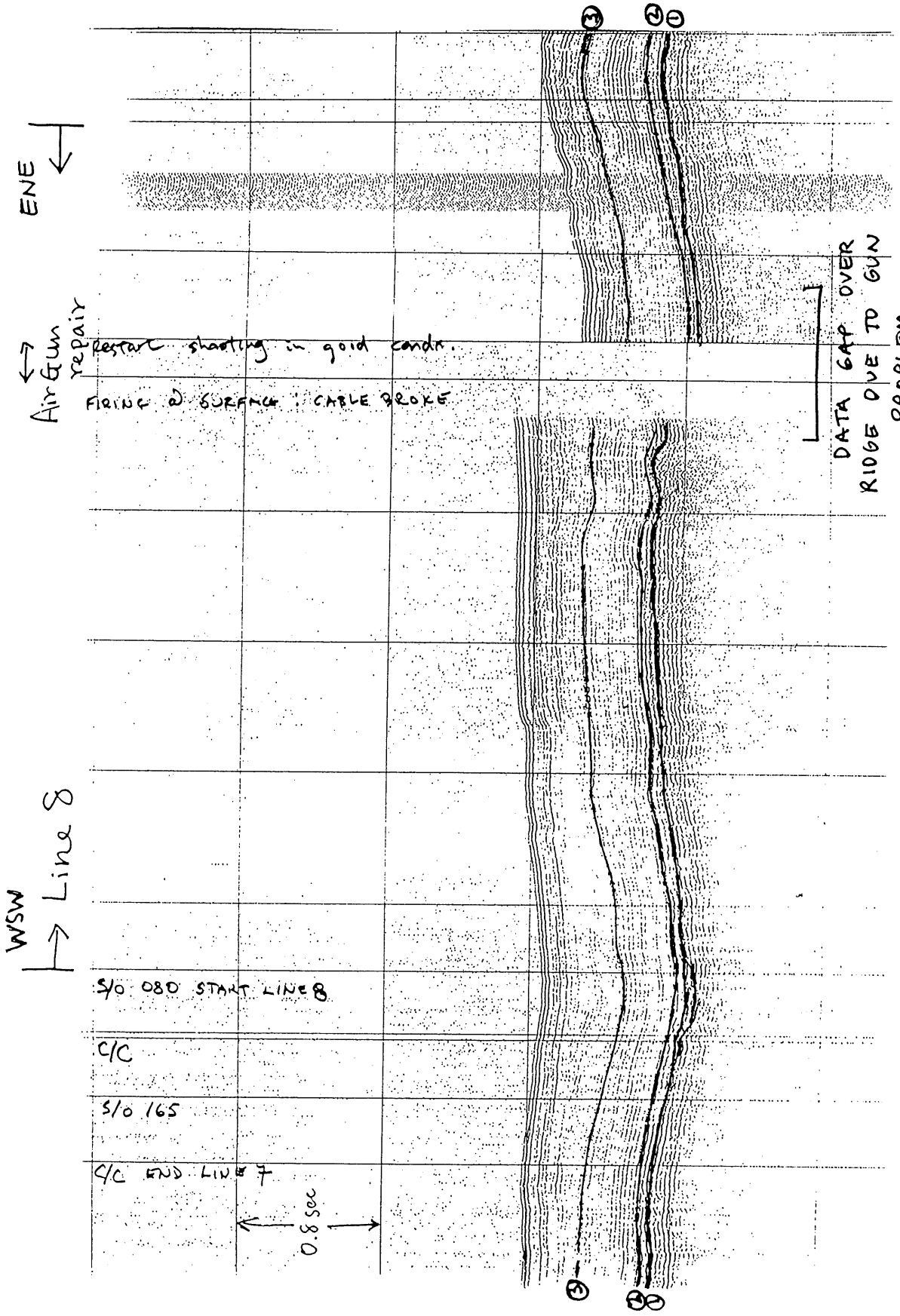
ENE
Air Gun repair
Restart shooting in good condx.
FIRING @ SURFACE : CABLE BROKE
DATA GAP OVER RIDGE DUE TO GUN PROBLEM
WSW
Line 8
S/O 080 START LINE 8
C/C
S/O 165
C/C END LINE 7
0.8 sec

LINE 8

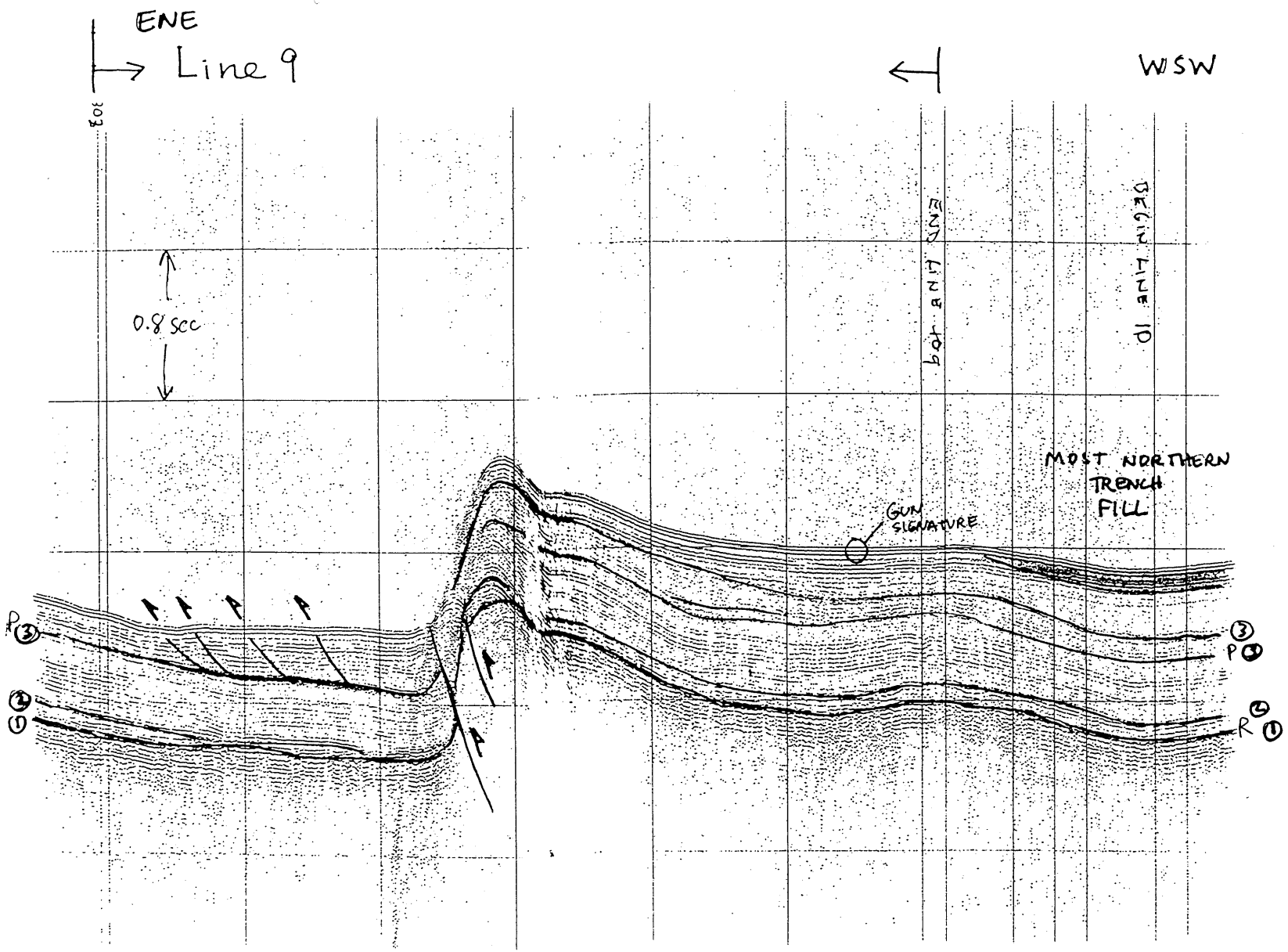
ENE
Line 9
WSW
303
0.8 sec
END LINE 304
BEGIN LINE 10
MOST NORTHERN TRENCH FILL
GUN SIGNATURE
P
R
3
2
1

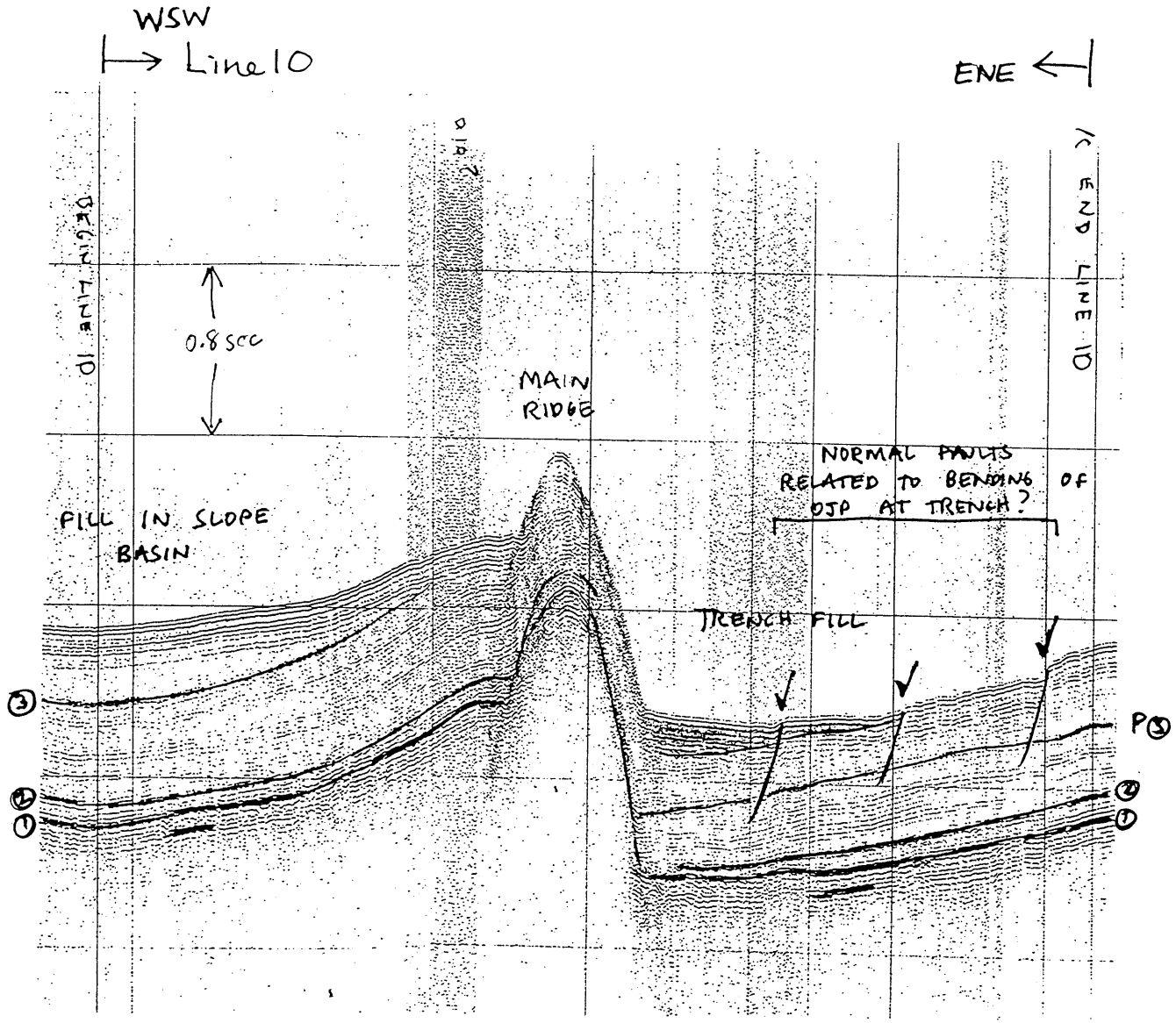
WSW
Line 10
ENE
BEGIN LINE 10
0.8 sec
MAIN RIDGE
END LINE 10
FILL IN SLOPE BASIN
NORMAL FAULTS RELATED TO BENDING OF OJP AT TRENCH?
TRENCH FILL
P
3
2
1

LINE 10

WSW
DATA GAP - RECORDER OVER-RERTED?
FILL
A
A'
monitor CH → 8
shoot stop chk leakage → seems ok
resume on 0316Z
FILL
0.8 sec
260 BEGIN LINE 11
ENE
Line 11

LINE 11

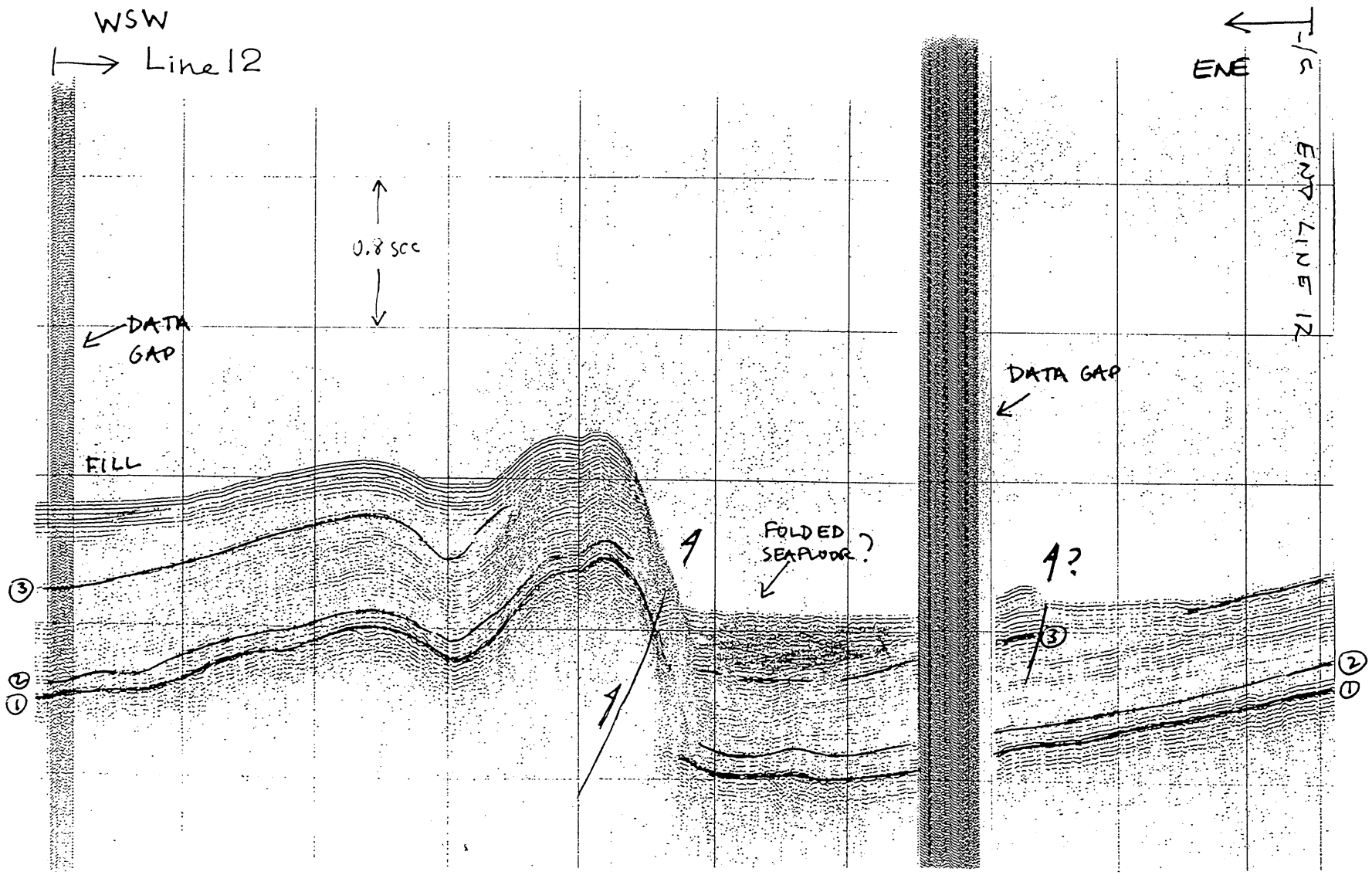
WSW
Line 12
0.8 sec
DATA GAP
FILL
FOLDED SEAFLOOR?
DATA GAP
ENE
END LINE 12
3
2
1

LINE 12

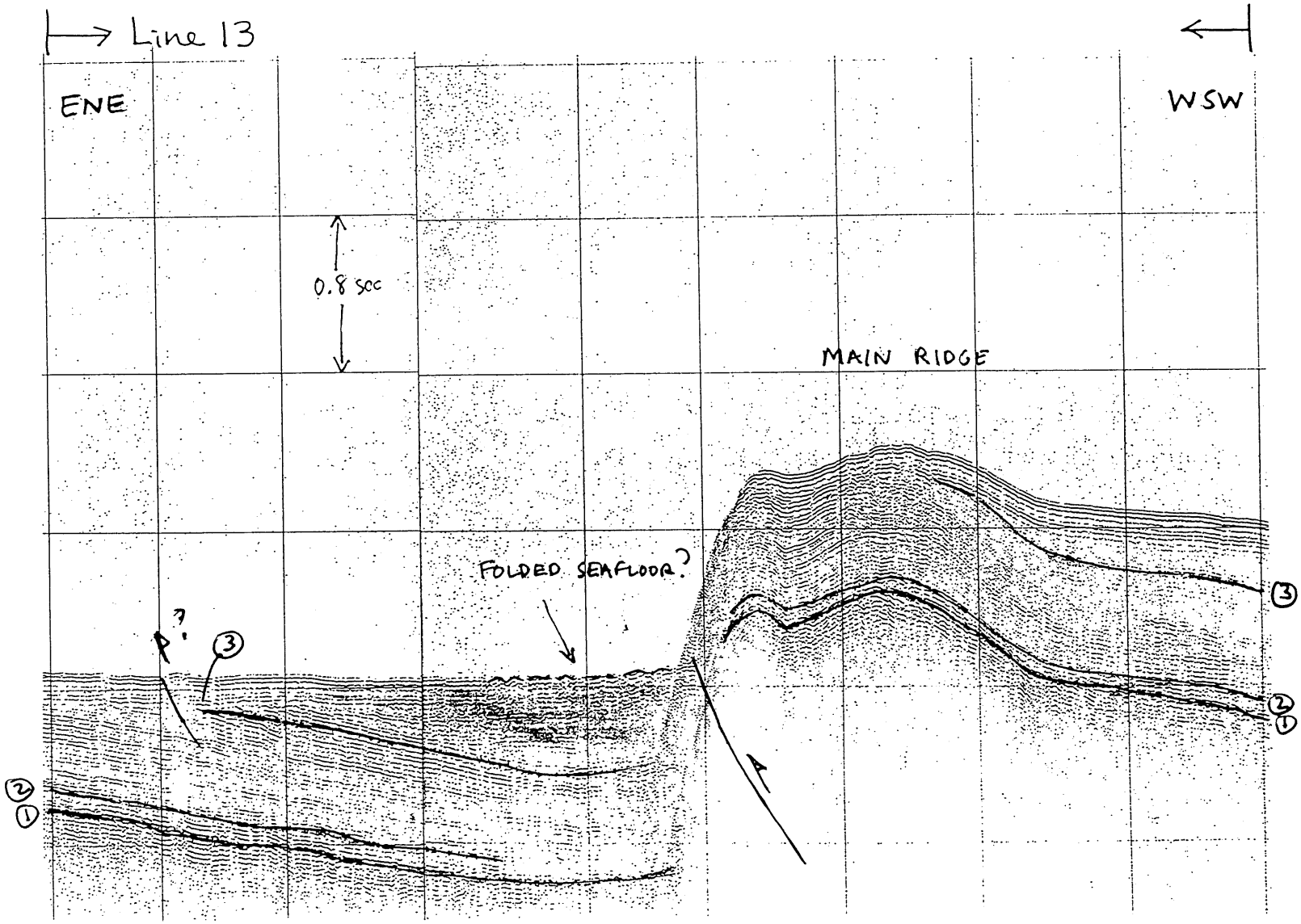

LINE 13

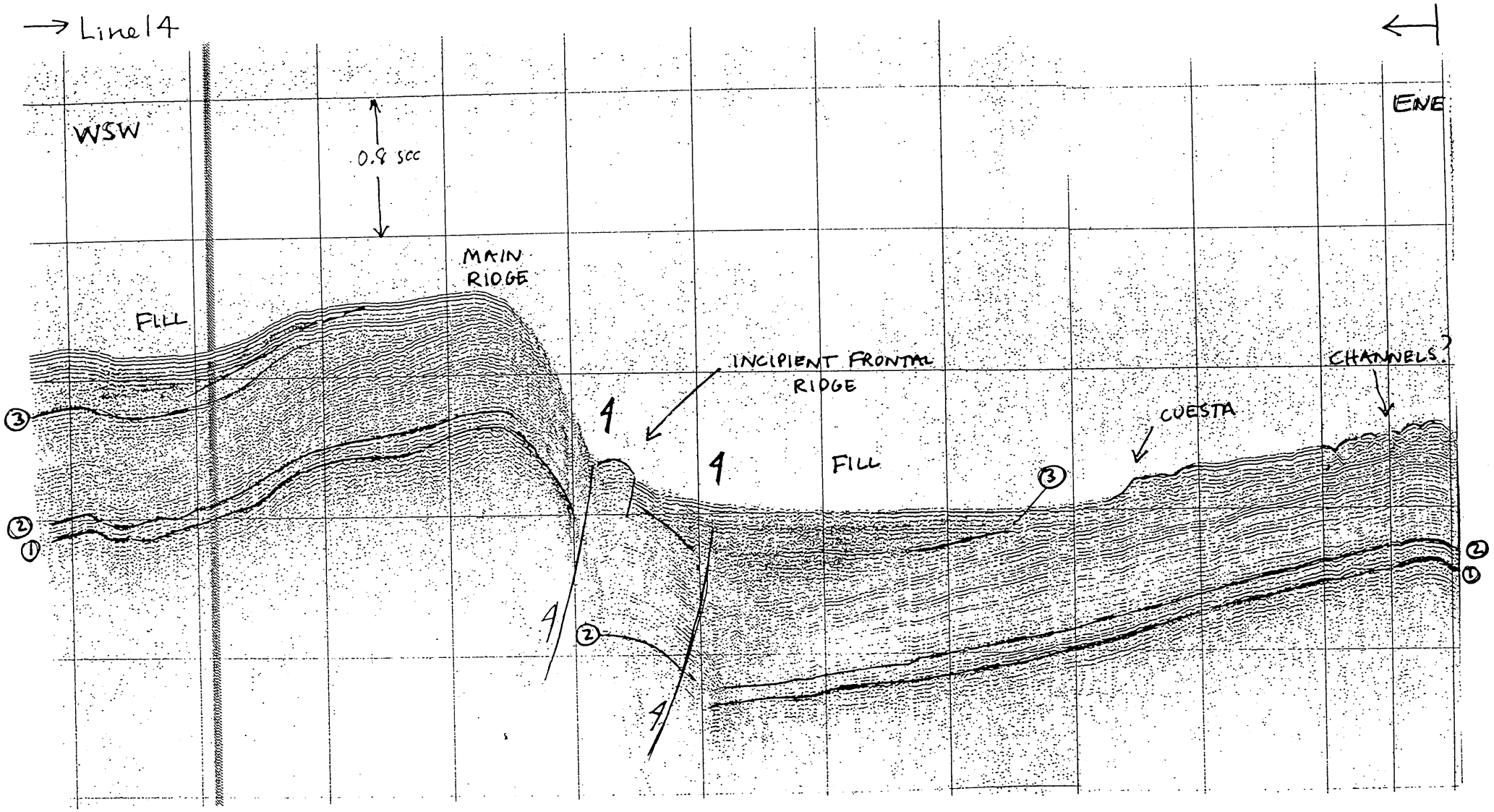
→ Line 14
←
WSW
ENE
0.8 sec
MAIN RIDGE
FILL
INCIPIENT FRONTAL RIDGE
CHANNELS?
CUESTA
FILL
3
2
1
4

LINE 14

WSW
FILL
MAIN RIDGE
BREAKAWAY?
SLUMP?
FRONTAL RIDGE
0.9 sec
FILL
FOLDS
CUESTAS?
BEGIN LINE 15
ENE
Line 15

LINE 15

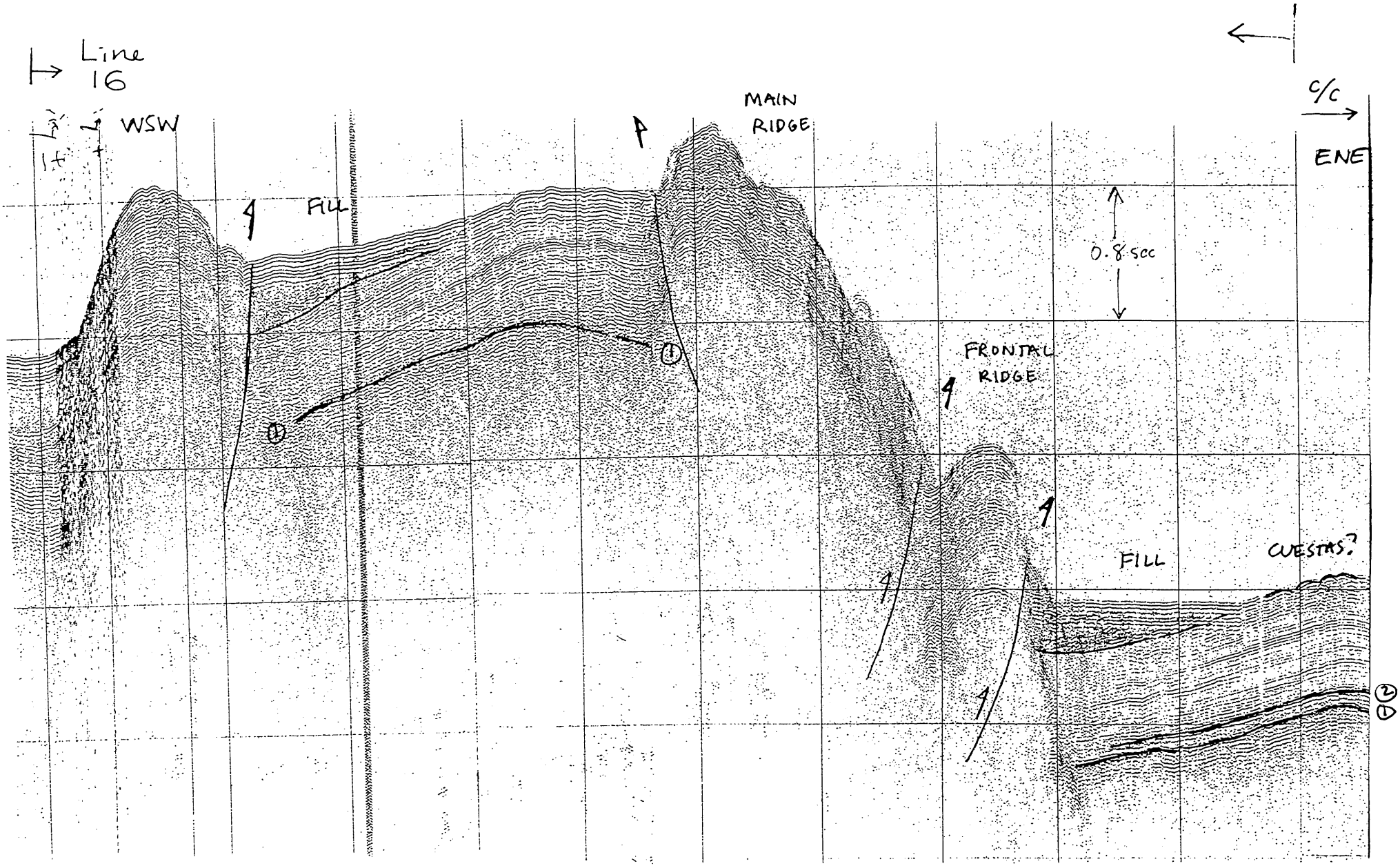
Line 16
WSW
MAIN RIDGE
C/C
ENE
FILL
0.8 sec
FRONTAL RIDGE
FILL
CUESTAS?
2
1

LINE 16

F1 - ACQUISITION MENU

ACQUISITION PARAMETERS		
Total Channels	:	24
Number of Auxes	:	0
SamPle Rate	:	2.0
Record LenGth (ms)	:	7500
TB Offset (ms)	:	0
Stack Parameters		1 STACK
Pre-View Stack	:	No
Correlation Mode		Raw Mode
Noise EditinG Pa		
Filter Parameter		
TriGGer Level (m		
Automatic Re-ARM		
Stack Delay (ms)		
Shot Pt Delay(ms)	:	0
(TB) TriGGer TyPe	:	TTL Edge
Arm ReQuest Para		Arm ReQ Para
TriGGer Parameters		TriG Para

OYO MINIVIB PARAMETERS		
SweeP TyPe	:	Linear SwP
SweeP LenGth (ms)	:	1024
TaPer LenGth (ms)	:	200
AmPlitude (%)	:	10
No. of FreQ Zones	:	1
FliP Polarity	:	No FliP
Start FreQuency	:	30.0000

Low Cut FreQuency(Hz)	:	3.0000
Low Cut SloPe(dB/Oct)	:	6 dB/Oct
Extended CutOff FreQ	:	No

FreQ	dB/oc	dB/Hz
00.00	0.0	0.00

F1 - ACQUISITION MENU

ACQUISITION PARAMETERS		
Total Channels	:	24
Number of Auxes	:	0
SamPle Rate	:	2.0
Record LenGth (ms)	:	7500
TB Offset (ms)	:	0
Stack Parameters		1 STACK
Pre-View Stack	:	No
Correlation Mode		Raw Mode
Noise EditinG Para		No EditinG
Filter Parameters		Filter
TriGGer Level (mV)	:	255
Automatic Re-ARM	:	Automatic
Stack Delay (ms)	:	0
Shot Pt Delay(ms)	:	0
(TB) TriGGer TyPe	:	TTL Edge
Arm ReQuest Para		Arm ReQ Para
TriGGer Parameters		TriG Para

OYO MINIVIB PARAMETERS		
SweeP TyPe	:	Linear SwP
SweeP LenGth (ms)	:	1024
TaPer LenGth (ms)	:	200
AmPlitude (%)	:	10
No. of FreQ Zones	:	1
FliP Polarity	:	No FliP
Start FreQuency	:	30.0000

Zone	St FreQ	End FreQ	dB/oc	dB/Hz
1	30.00	100.00	0.0	0.00

SEISMIC ACQUISITION PARAMETERS – KH-98-1

Table 1

F2 - SPREAD PARAMETER MENU

LINE CONFIGURATION

Unit (feet/meter) :	Meter
Number of lines :	1
Line to Line Dist :	1
Sta to Sta Dist :	1
Station Interval :	1
Line 1 Number :	1
Line 1 First sta-no:	1

ROLL PARAMETERS

Automatic Roll :	No
Shot Pt Interval :	0
Receiver Interval :	0
Rolling On (Y/N) :	No
Shot Pt Line Number :	1
Shot Pt Line Offset :	0.0000
Shot Pt Station No. :	1
Shot Pt Station Offset :	0.0000
GAP station no. (LOW) :	0
GAP station no. (HIGH) :	0
GAP stations connected :	Yes
PreamP Gain radius :	0
First Active Sta Number:	1
Active Channels ***:	24
Max Active Channels :	48

F3 - PLOT PARAMETER MENU

PLOT PARAMETERS

Plot Start Chan :	1
Increment By :	1
Total Seis Chans:	24
Number of Aux :	0
Polarity :	Positive
Plot Offset (ms):	0
Plot Length (ms):	7500
Chart Length :	1 to 1
Plot Format :	Time
Auto SPacing :	Yes
Trace Per Inch :	1
Sig Attenuation :	0db
Trace OverlaP :	1
Plot Mode :	Variable
Plot Interval :	0
Screen DisPlay :	ON
Plot Header :	Print None
Plotter TyPe :	INTERNAL

FILTER PARAMETERS

LoCut Filter(Frq,Sl):	No
HiCut Filter(Frq,Sl):	No
Notch1 Filtr(Fr,B,H):	No
Notch2 Filtr(Fr,B,H):	No
Notch3 Filtr(Fr,B,H):	No
AmPlitude SPectrum :	No
Enable Interval :	0

AGC PARAMETERS

Gain Control Method :	Fixed Gain
Fixed Gain [dB]:	0
Auxillary Gain [dB]:	0

F4 - STORAGE PARAMETER MENU

STORAGE PARAMETERS

Storage TyPe :	SCSI
File Number :	10535
Reel Number :	8
File Format :	SEGD 8048
Write Confirm :	No
Read After Write:	No

SAVE

OBSERVER LOG

Client : Team TAISKI
ComPany : Ocean Resarch Institute, Univ. of Tokyo
Job ID :
Observer:
Note : KH98-1 Ontong-Java Cruise
: North Choiseul
:
:
:
:
:

Table 2

SEISMIC DATA LOG — KH-98-1 (page 1/4)

Line	Date	Time(UT)	Latitude	Longitude	Depth	Rl	File	Comments
1	1/27/98	05:10:50	S 5 53.04	E 157 33.80	2610	1	1	Begin Shooting
		05:30:00	S 5 53.48	E 157 31.67	2529	1	116	
		05:31:30				1	125	Shot Stop
		05:33:50				1	126	Shot Restart
		05:34:40	S 5 53.59	E 157 31.10		1	131	
		06:00:00	S 5 54.13	E 157 28.18		1	283	
		06:30:00	S 5 54.79	E 157 24.86		1	462	
		07:00:00	S 5 55.48	E 157 21.45		1	643	
		07:30:00	S 5 58.63	E 157 20.59		1	870	
1	1/27/98	07:33:24	S 5 59.08	E 157 20.72		1		C/C L1
2	1/27/98	07:48:33	S 6 00.16	E 157 22.35		1	940	O/C L2
		07:51:28	S 6 00.14	E 157 22.73		1		Point Through
		08:00:00	S 6 00.03	E 157 23.94		1	1003	
		08:30:00	S 5 59.15	E 157 27.75	2715	1	1183	
		09:00:00	S 5 58.33	E 157 31.78	2710	1	1364	
		09:30:01	S 5 57.60	E 157 35.53	2700	1	1543	
		10:00:00	S 5 56.84	E 157 39.46	2655	1	1723	
		10:30:08	S 5 56.09	E 157 43.30	2650	1	1903	
		11:00:00	S 5 55.34	E 157 47.18	2750	1	2083	
2	1/27/98	11:21:00	S 5 54.64	E 157 50.73		1		C/C L2
		11:30:28	S 5 54.58	E 157 51.12	2725	1	2282	
		12:00:00	S 5 57.31	E 157 53.00	2770	1	2448	
3	1/27/98	12:22:33	S 5 59.28	E 157 52.28	2825	1	2586	O/C L3
		12:30:00	S 5 59.42	E 157 51.32	2825	1	2627	
		13:00:00	S 6 00.17	E 157 47.95	2875	1	2803	
		13:30:00	S 6 00.82	E 157 44.53	2840	1	2983	
		14:00:00	S 6 01.51	E 157 41.16	2825	1	3163	
		14:30:00	S 6 02.18	E 157 37.82	2850	1	3343	
		15:00:00	S 6 02.80	E 157 34.58	2840	1	3523	
		15:30:00	S 6 03.46	E 157 31.29	2790	1	3703	
		16:00:00	S 6 04.09	E 157 28.01	2815	1	3883	
3	1/27/98	16:22:30	S 6 04.56	E 157 25.62		1	3949	C/C L3
	1/27/98	16:44:10	S 6 06.97	E 157 25.12		2	3951	Tape Change
		17:00:00	S 6 08.87	E 157 23.94	2940	2	4046	
4	1/27/98	17:11:00	S 6 09.11	E 157 27.43	2970	2		O/C L4
		17:12:40				2	4122	
		17:30:00	S 6 08.66	E 157 29.96	2950	2	4226	
		18:00:50	S 6 07.86	E 157 33.99	2920	2	4411	
		18:30:00	S 6 07.05	E 157 38.00	2900	2	4586	
		19:00:00	S 6 06.24	E 157 41.95	2930	2	4766	
		19:30:00	S 6 05.44	E 157 45.94	2990	2	4946	
		20:00:00	S 6 04.68	E 157 49.97	2975	2	5126	
		20:30:00	S 6 03.89	E 157 54.00	2970	2	5306	
4	1/27/98	20:45:09	S 6 03.47	E 157 56.01	2975	2	5402	C/C L4
		21:00:00	S 6 04.45	E 157 57.59	2180	2	5486	
		21:30:00	S 6 07.92	E 157 57.88	3080	2	5666	
5	1/27/98	21:35:17	S 6 08.18	E 157 57.35	3100	2	5697	O/C L5
		22:00:00	S 6 08.81	E 157 54.70	3145	2	5846	
		22:30:00	S 6 09.46	E 157 51.46	2980	2	6026	
		23:00:00	S 6 10.08	E 157 48.18	2810	2	6206	
		23:30:00	S 6 10.70	E 157 44.95	2960	2	6386	
	1/28/98	00:00:00	S 6 11.34	E 157 41.65	2975	2	6566	
		00:30:00	S 6 11.96	E 157 38.42	2980	2	6746	
5	1/28/98	01:04:10	S 6 12.65	E 157 34.74	3050	2	6951	C/C L5
	1/28/98	01:18:10	S 6 14.01	E 157 34.00		2	7035	
		01:30:00	S 6 15.49	E 157 34.47	3150	3		Tape Change
		01:30:30	S 6 15.49	E 157 34.47		3	7036	
		01:32:10				3	7038	
6	1/28/98	01:53:10	S 6 17.71	E 157 36.25	3175	3		O/C L6, DAS-1 Trouble
		02:00:00	S 6 17.41	E 157 37.12	3175	3		
		02:13:30	S 6 17.89	E 157 39.02	3150	3	7036	DAS-1 Green
		02:30:00	S 6 16.40	E 157 41.19	3050	3	7135	
		03:00:00	S 6 15.55	E 157 45.32	3125	3	7315	
		03:30:00	S 6 16.69	E 157 49.47	2985	3	7495	
		04:00:00	S 6 13.88	E 157 53.61	3050	3	7675	
		04:30:00	S 6 13.05	E 157 57.76	2840	3	7855	
		05:00:00	S 6 12.22	E 158 01.84	3230	3	8035	
		05:31:30	S 6 11.40	E 158 06.07	3140	3	8224	

(4 pages)

Table 2

Line	Date	Time(UT)	Latitude	Longitude	Depth	Rl	File	Comments
		06:00:00	S 6 10.68	E 158 09.85	3100	3	8395	
6	1/28/98	06:25:10	S 6 10.04	E 158 13.18	3050	3	8545	C/C L6
		06:31:00	S 6 10.16	E 158 14.00		3	8581	
		07:00:00	S 6 13.36	E 158 15.33	3115	3	8755	
7	1/28/98	07:13:53	S 6 14.46	E 158 15.43	2180	3	8838	O/C L7
		07:30:00	S 6 15.07	E 158 12.83	3230	3	8935	
		08:00:00	S 6 15.71	E 158 09.65	3280	3	9115	
		08:30:15	S 6 16.41	E 158 06.03	3225	3	9295	
		09:00:00	S 6 17.11	E 158 02.52	2900	3	9475	
		09:30:00	S 6 17.79	E 157 58.98	3050	3	9655	
		10:00:00	S 6 18.50	E 157 55.41	3055	3	9835	
		10:30:00	S 6 19.21	E 157 51.79	3060	3	10015	
		11:00:00	S 6 19.91	E 157 48.14	3200	3	10195	
7	1/28/98	11:30:00	S 6 20.63	E 157 44.50	3175	3	10375	C/C L7
	1/28/98	11:40:50	S 6 21.57	E 157 43.60		4	10407	Tape Change
8	1/28/98	12:14:18	S 6 25.16	E 157 46.11	3500	4	10478	O/C L8
		12:30:00	S 6 24.85	E 157 48.48	3225	4	10573	
		13:00:00	S 6 23.99	E 157 52.79	3175	4	10753	
		13:30:00	S 6 23.10	E 157 57.12	3120	4	10933	
		14:00:00	S 6 22.23	E 158 01.44	3120	4	11107	
		14:30:00	S 6 21.38	E 158 05.73	3040	4	11293	
		14:39:20	S 6 21.13	E 158 7.10		4	11349	gun shot stop
		15:00:00	S 6 19.29	E 158 16.42	3330			
		15:42:20	S 6 19.78	E 158 13.91	3360	4	11353	gun shot restart
		16:30:00	S 6 18.40	E 158 20.86	3230	4	11638	
8	1/28/98	16:35:12	S 6 18.26	E 158 21.62	3230	4	11670	C/C
		17:00:00	S 6 20.46	E 158 23.71	3270	4	11879	
9	1/28/98	17:28:30	S 6 23.01	E 158 22.41		4	11990	O/C L9
		17:30:00	S 6 23.08	E 158 22.22	3440			
		18:01:00	S 6 23.85	E 158 18.71	3490	4	12185	
		18:32:00	S 6 24.52	E 158 15.19	3505	4	12371	
		19:00:00	S 6 25.13	E 158 11.98	2870	4	12539	
		19:30:00	S 6 25.81	E 158 8.57	3120	4	12719	
		20:00:00	S 6 26.47	E 158 5.22	3200	4	12899	
		20:30:00	S 6 27.08	E 158 1.89	3200	4	13079	
9	1/28/98	20:35:20	S 6 27.23	E 158 1.27	3190	4	13111	C/C
		21:00:00	S 6 30.06	E 158 0.88	3235	4	13259	
10	1/28/98	21:22:19	S 6 32.17	E 158 02.99	3265	4	13392	O/C L10
		21:30:00	S 6 31.84	E 158 04.12	3055	4	13439	
		22:00:00	S 6 30.77	E 158 08.49	3190	4	13619	
		22:30:00	S 6 29.84	E 158 12.99	2980	4	13799	
		23:00:00	S 6 28.96	E 158 17.58	2975	4	13939	
		23:30:00	S 6 28.06	E 158 22.16	3580	4	14159	
	1/29/98	00:00:00	S 6 27.15	E 158 26.75	3540	4	14339	
		00:28:00				4	14500	Tape Eject
		00:30:00	S 6 26.25	E 158 31.37	3400			Shot Stop
	1/29/98	00:35:30				5	14501	Tape Change, Shot Start
10	1/29/98	00:45:09	S 6 25.76	E 158 33.79	3275	5	14558	C/C L10
		01:00:01	S 6 26.81	E 158 35.27	3300	5	14648	
		01:30:00	S 6 28.95	E 158 35.47	3525	5	14828	
11	1/29/98	01:32:45	S 6 30.36	E 158 35.16	3550	5	14844	O/C L11
		02:00:00	S 6 31.05	E 158 32.17	3650	5	15008	
		02:30:00	S 6 31.74	E 158 28.76	3650	5	15188	
		03:00:00	S 6 32.41	E 158 25.27	3320	5	15368	
		03:11:20	S 6 32.69	E 158 2?.92		5	15436	Shot Stop (Air Check)
		03:16:30				5	15437	Shot Restart
		04:00:00	S 6 33.77	E 158 18.55	2860	5	15699	
		04:31:00	S 6 34.45	E 158 15.08	3195	5	15885	
		05:03:20	S 6 35.20	E 158 11.26	3250	5	818	
		05:10:00				5	1199	Shot Stop
		05:10:40	S 6 35.34	E 158 10.52				Shot Restart (record off)
11	1/29/98	05:35:38	S 6 37.02	E 158 08.73	3300			C/C 170 deg. L11
		06:00:19	S 6 40.03	E 158 10.37				DAS-1 Over Heat
		06:06:00	S 6 40.10	E 158 11.23				Shot Stop
12	1/29/98	06:06:40				6	1	DAS-1 Recovered, shot Restart,

Line	Date	Time(UT)	Latitude	Longitude	Depth	Rl	File	Comments
								Tape Change, O/C L12
		06:30:00	S 6 39.46	E 158 14.79	3290	6	1411	Odd File #
		07:04:00	S 6 38.47	E 158 19.80	3140	6	3442	Odd File #
		07:30:00	S 6 37.74	E 158 23.43	3225	6	5001	Odd File #
		08:00:00	S 6 36.91	E 158 27.60	3030	6	6801	Odd File #
		08:30:00	S 6 36.07	E 158 31.74	3720	6	8601	Odd File #
		09:00:00	S 6 35.25	E 158 35.90	3725	6	10401	Odd File #
		09:34:16	S 6 34.34	E 158 40.62	3650	6		Odd File #
		10:00:00	S 6 33.62	E 158 44.18	3660	6	14010	Odd File #
		10:30:00	S 6 32.84	E 158 48.29	3630	6	15811	Odd File #
12	1/29/98	10:45:05	S 6 32.44	E 158 50.40	3560	6	16701	C/C L12, Odd File #
		11:00:00	S 6 33.29	E 158 52.05	3630	6	17661	Odd File #
		11:30:00	S 6 36.71	E 158 52.26		6	1882	Odd File #
13	1/29/98	11:39:43	S 6 37.07	E 158 51.16	3730	6	1999	O/C L13
		12:00:00	S 6 37.53	E 158 48.74	3750	6	2121	
		12:30:00	S 6 38.33	E 158 45.16	3750	6	2301	
		13:00:00	S 6 39.09	E 158 41.60	3770	6	2481	
		13:30:00	S 6 39.90	E 158 37.77	3750	6	2661	
		14:00:00	S 6 40.61	E 158 34.08	3710	6	2841	
		14:30:00	S 6 41.32	E 158 30.40	2930	6	3021	
		15:00:00	S 6 42.01	E 158 26.91	2950	6	3201	
		15:30:00	S 6 42.71	E 158 23.41	3130	6	3381	
13	1/29/98	16:00:00	S 6 43.36	E 158 19.94	3180	6	3561	C/C L13
		16:30:00	S 6 44.86	E 158 19.82	3110	6	3741	
14	1/29/98	16:47:20	S 6 47.93	E 158 21.94	3090	6	3845	O/C L14
		17:02:00	S 6 47.64	E 158 23.91	3060	6	3933	
		17:30:00	S 6 46.89	E 158 27.72	3090	6	4096	Tape Eject
	1/29/98	17:35:00				7	4097	Tape Start
		18:00:00	S 6 46.09	E 158 31.76	2900	7	4247	
		18:30:40	S 6 45.33	E 158 35.75	2840	7	4431	
		19:00:00	S 6 44.58	E 158 39.55	3380	7	4607	
		19:30:40	S 6 43.81	E 158 43.42	3250	7	4787	
		20:00:00	S 6 43.06	E 158 47.26	3780	7	4967	
		20:30:01	S 6 42.31	E 158 51.13	3790	7	5147	
		21:00:00	S 6 41.54	E 158 55.08	3775	7	5327	
		21:30:00	S 6 40.79	E 158 58.87	3505	7	5507	
		22:00:00	S 6 40.08	E 159 02.74	3545	7	5687	
14	1/29/98	22:15:08	S 6 40.79	E 159 04.67	3475	7	5777	C/C L14
		22:30:00	S 6 40.68	E 159 06.06	3475	7	5867	
		23:00:00	S 6 44.18	E 159 05.71	3700	7	6047	
15	1/29/98	23:04:54	S 6 44.36	E 159 05.12	3675	7	6075	O/C L15
		23:30:00	S 6 45.22	E 159 01.97	3810	7	6227	
	1/30/98	00:00:00	S 6 45.95	E 158 58.22	3820	7	6407	
		00:30:00	S 6 46.68	E 158 54.47	3780	7	6587	
		01:00:00	S 6 47.40	E 158 50.73	3275	7	6767	
		01:30:00	S 6 48.10	E 158 47.07	3420	7	6947	
		02:00:00	S 6 48.80	E 158 43.44	2710	7	7126	
		02:30:00	S 6 49.51	E 158 39.88	2370	7	7306	
		03:00:00	S 6 50.21	E 158 36.19	2500	7	7486	
15	1/30/98	03:30:00	S 6 50.97	E 158 32.32	2630	7	7666	C/C L15
		04:00:00	S 6 54.48	E 158 31.88	2210	7	7846	
16	1/30/98	04:20:00	S 6 55.47	E 158 34.06	1980	7	7966	O/C L16
		04:30:00	S 6 55.36	E 158 35.34	2190	7	8026	
		05:00:00	S 6 54.59	E 158 39.37				Tape Change
		05:05:50	S 6 54.59	E 158 39.37		8	8229	
		05:31:00	S 6 53.73	E 158 43.60	2100	8	8379	
		06:00:00	S 6 52.97	E 158 47.46	1980	8	8553	
		06:30:00	S 6 52.21	E 158 51.38	1700	8	8733	
		07:00:00	S 6 51.51	E 158 55.17	3275	8	8913	
		07:30:00	S 6 50.76	E 158 59.12	3225	8	9093	
		08:00:14	S 6 49.97	E 159 03.06	3810	8	9273	
		08:30:00	S 6 49.21	E 159 06.96	3855	8	9453	
		09:00:14	S 6 48.43	E 159 10.95	3775	8	9633	
16	1/30/98	09:04:50	S 6 48.31	E 159 11.58	3750	8	9662	C/C L16
		09:30:00	S 6 50.52	E 159 12.98	3850	8	9813	
		10:00:14	S 6 53.52	E 159 10.97	3875	8	9993	
		10:30:00	S 6 53.09	E 159 07.84	3860	8	10173	

Line	Date	Time(UT)	Latitude	Longitude	Depth	Rl	File	Comments
17	1/30/98	10:39:37	S 6 52.08	E 159 07.34	3875	8	10230	O/C L17
		11:00:06	S 6 49.62	E 159 06.94	3860	8	10353	
		11:03:19	S 6 49.23	E 159 06.87	3850	8	10372	Passed Though the Base Point
		11:30:00	S 6 46.03	E 159 06.28	3770	8	10533	End Shooting

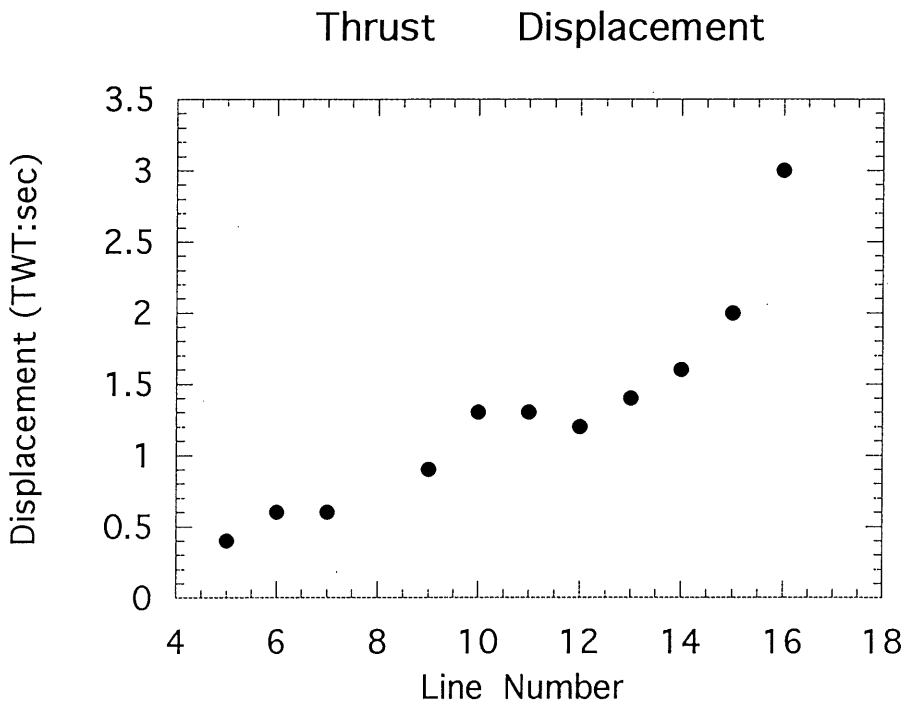
Thrust Displacement
Displacement (TWT:sec)
3.5
3
2.5
2
1.5
1
0.5
0
4
6
8
10
12
14
16
18
Line Number

Cruise report HK 98 - Leg 1 - January 16th - February 3rd 1998

Description of characteristic 3.5 kHz profiles across the Ontong Java Plateau (OJP) and northern Solomon Trench

Wietze van der Werff (STA post-doc fellow, Geological Survey of Japan)

Seabottom profiling (3.5 kHz) has been recorded continuously during Leg 1 of HK 98. The profiles provide information about the nature of recent sedimentation processes and tectonic activity. In addition, the acoustic signature reveals the morphology, structure and texture of the seabottom. During Leg 1, research focused on the detection of magnetic anomalies in the Lyra Basin, OBS deployment on top of the OJP, and side-scan sonar and single-channel seismic profiling along the northern Solomon Trench. As a consequence, 3.5 kHz profiles cover at least seven distinct structural areas of which the acoustic characteristics are described below (Figures 1-15). The names and position of profile Sections L7-L15 (Figures 7-15) conform with the single-channel profiles discussed in a different section. In chronological order, the provinces comprise:

A) The northwestern slope of the Ontong Java Plateau
B) The Ontong Java Plateau
C) The Lyra Basin (west of the Ontong Java Plateau)
D) The southern slope of the Ontong Java Plateau
E) The North Solomon Trench, the Frontal Thrust, and the Slope Basin

The 3.5 kHz profiles have a horizontal line spacing of 150 m. The vertical lines delineate 15 minute intervals. Time (GMT) and position (GPS) have been annotated along these intervals.

Description

Ad A) The northwestern slope of the Ontong Java Plateau (Figure 1)

The slope of OJP is underlain by weakly reflective, undulating reflectors. The seabottom is characterized by a highly reflective topography possibly which is incised by canyons. The maximum penetration is about 65 meters.

Ad B) The Ontong Java Plateau (Figures 2,4)

The section of the 3.5 kHz profile illustrates the top of the northern Ontong Java Plateau (Figure 2). The OJP is characterized by a rugged topography deeply incised by valleys or submarine canyons (260 meters of relief). Acoustic penetration reaches shallow depths of less than 40 meters. Locally, slightly deformed, low amplitude reflectors are observed. Most of the OJP is characterized by a highly reflective seabottom. The rugged seabottom may be the result of volcanic activity. The southern OJP is characterized by a relatively flat surface incised by wide and shallow channels (Figure 4). The acoustic signal is almost completely reflected resulting in one continuous high amplitude seabottom reflector.

AD C) The Lyra Basin (Figure 3).

The Lyra Basin is underlain by rather angular ridges with heights of up to 300 meters. These are overlain by weakly reflective, low amplitude parallel reflectors. The acoustic penetration reaches a maximum depth of 40 meters. The reflectors appear to be offset by small faults along the "eastern" flank of the major ridge.

Ad D) The southern slope of the Ontong Java Plateau

The southern slope of the Ontong Java Plateau consists of a relatively steep slope underlain by continuous, parallel, high amplitude reflectors. The acoustic penetration is up to 30 meters. Half way the slope, strata are deformed due to slumping.

AD E) The northern Solomons Trench, Frontal Thrust and Slope Basin(Figures 6-15)

Frontal thrust development is discussed from WNW to ESE.

The trench is characterized by a seismically transparent facies with a maximum thickness of 60 meters. The trench deposits overlie and onlap a highly reflective acoustic basement (Figure 6)". The seabottom is characterized by an irregular high amplitude reflector. This may be related to the coarse grained texture of trench-fill turbidites. The frontal thrust is underlain by continuous, even bedded, high amplitude reflectors. Along the lower inner trench slope, the strata are deformed possibly indicating slump activity The acoustic penetration is about 70 meters.

Profile L14 provides another example of the trench and thrust front (Figure 7). The lower slope of the thrust front is overlain by an acoustically incoherent slump mass. The trench itself is characterized by a blocky, irregular highly reflective seabottom which most likely is underlain by turbidite deposits transported from both the inner and outer trench slopes. Acoustic penetration is limited to 20 meters.

Profile L-6 illustrates the frontal thrust. The trench is located to the right (Figure 8). The thrust is characterized by an apparent offset of approximately 520 meters. The seismic signature of the thrust is characterized by abundant diffraction hyperbolae suggesting a rugged and possibly tectonically deformed surface. A steep scarp with a relief of 150 m located along the left side of the profile may suggest the presence of a backthrust. Folded and weakly stratified sediments occur on top of the thrust. These deposits have a minimum thickness of 30 m. They probably extend into the slope basin where continuous parallel refectors are identified which are characterized by a comparable thickness.

Profile L-7 is very similar to Figure 8 but appears to be less deformed (Figure 9A). The frontal thrust is characterized by various diffraction hyperbolae and a highly reflective surface. The acoustic penetration is not so deep. The backthrust region (Figure 9B) is less deformed in comparison with Figure 8. The offset with the slope basin comprises approximately 150 m. The backthrust is slightly deformed and characterized by two open folds and a number of faults. The sediments covering the thrust have a minimum thickness of about 30 meter (the acoustic penetration). They comprise, continuous, even bedded, low amplitude reflectors which extend across the backthrust towards the north.

Profile L-9 shows several continuous high amplitude reflectors along the back of the frontal thrust (Figure 10). The thrust accomodates an uplift of 300 m which resulted in tilting of the basement. Maximum acoustic penetration is up to 50 m. The profile shows thinning of the sediments towards the frontal thrust where they obtain a minimum thickness of 10 meters. These deposits thicken towards the slope basin these where they attain a thickness of 50 meters. This may suggest that the recently formed thrust represents an important source area.

Profile L-11 probably illustrates a major backthrust as indicated by the steep slope which indicates an offset of 500 m (Figure 11). The slope basin is characterized by a diverging reflection configuration suggesting sedimentation derived from the backthrust. Maximum acoustic penetration below the slope basin comprises 50 m, which thins to about 15 m near the backthrust. The backthrust itself is highly reflective and acoustic penetation is low.

Profile L-12 illustrates a detail of the northern Solomon Trench (Figure 12). This part of the trench is characterized by a rough seabottom topography and a seismically amorphous slump block with a height of 150 m. This "cobble stone" topography probably relates to the presence of coarse terrigenous debrisflows and turbidite deposits. The acoustic penetration is up to 15 meters.

Profile L-13 illustrates the top of the backthrust (Figure 13). The profile shows a slope basin characterized by a series of high amplitude discontinuous reflectors which are tilted towards the thrust. The top of the thrust is underlain by a irregular bottom topography probably resulting from compressional tectonic deformation.

Profile L-14 shows that slope steepening resulted in slumping which is indicated by the presence of refraction hyperbolae along the base of the slope (Figure 14). This profile indicates mass flow processes which suggest that slope basin sedimentation initially can be controlled by source areas near the deformation front. The slope basin is characterized by a highly reflective surface that might indicate the presence of lag deposits.

Figure 15. Section of 3.5 kHz Profile L-15. For legend see Profile 1. Profile L-15 illustrates the back slope of the frontal thrust (Figure 15). The section is characterized by the widespread presence of diffraction hyperbolae along the slope. This may suggest a very rough topography

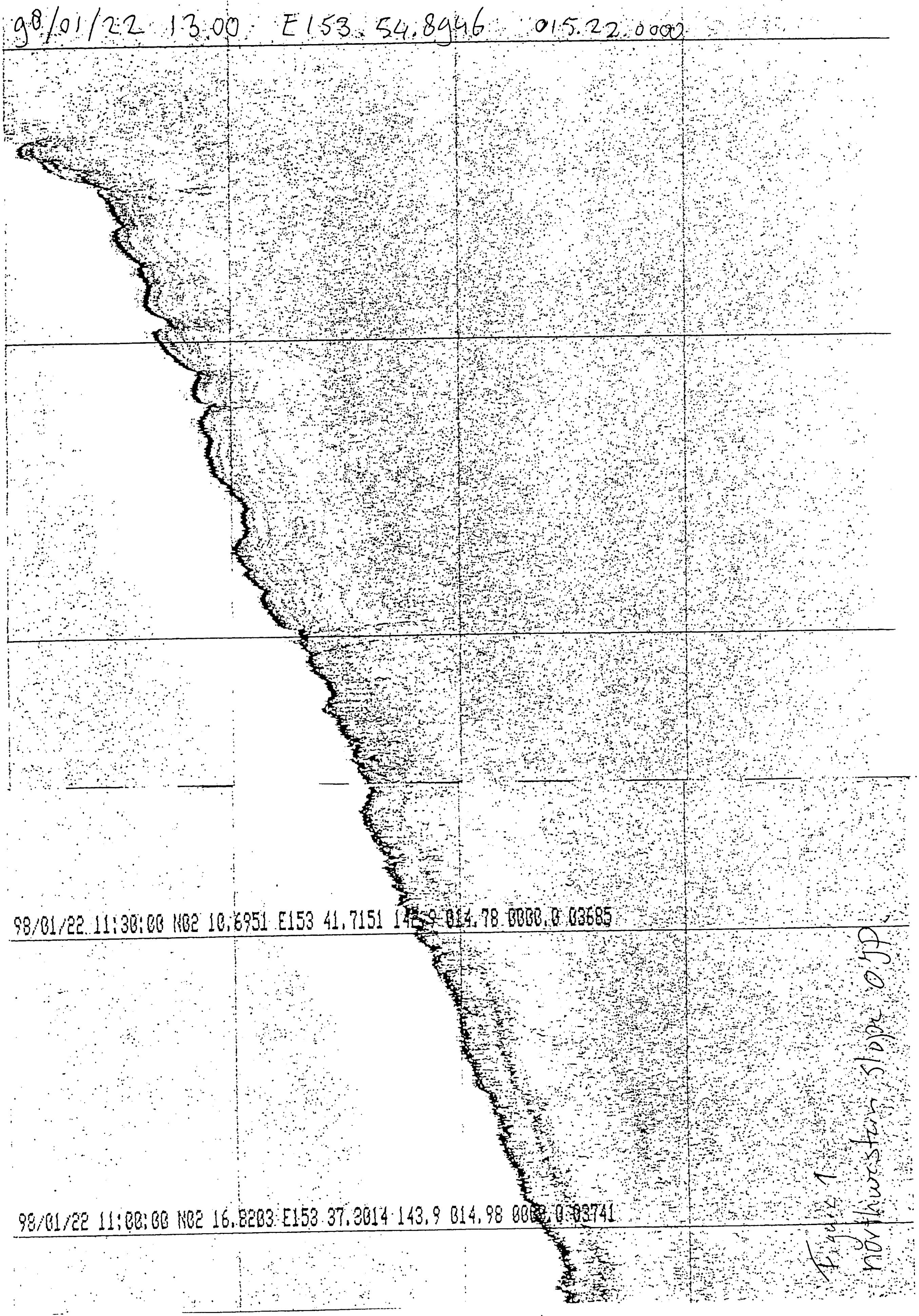

Fig. 1 northwestern slope OJP

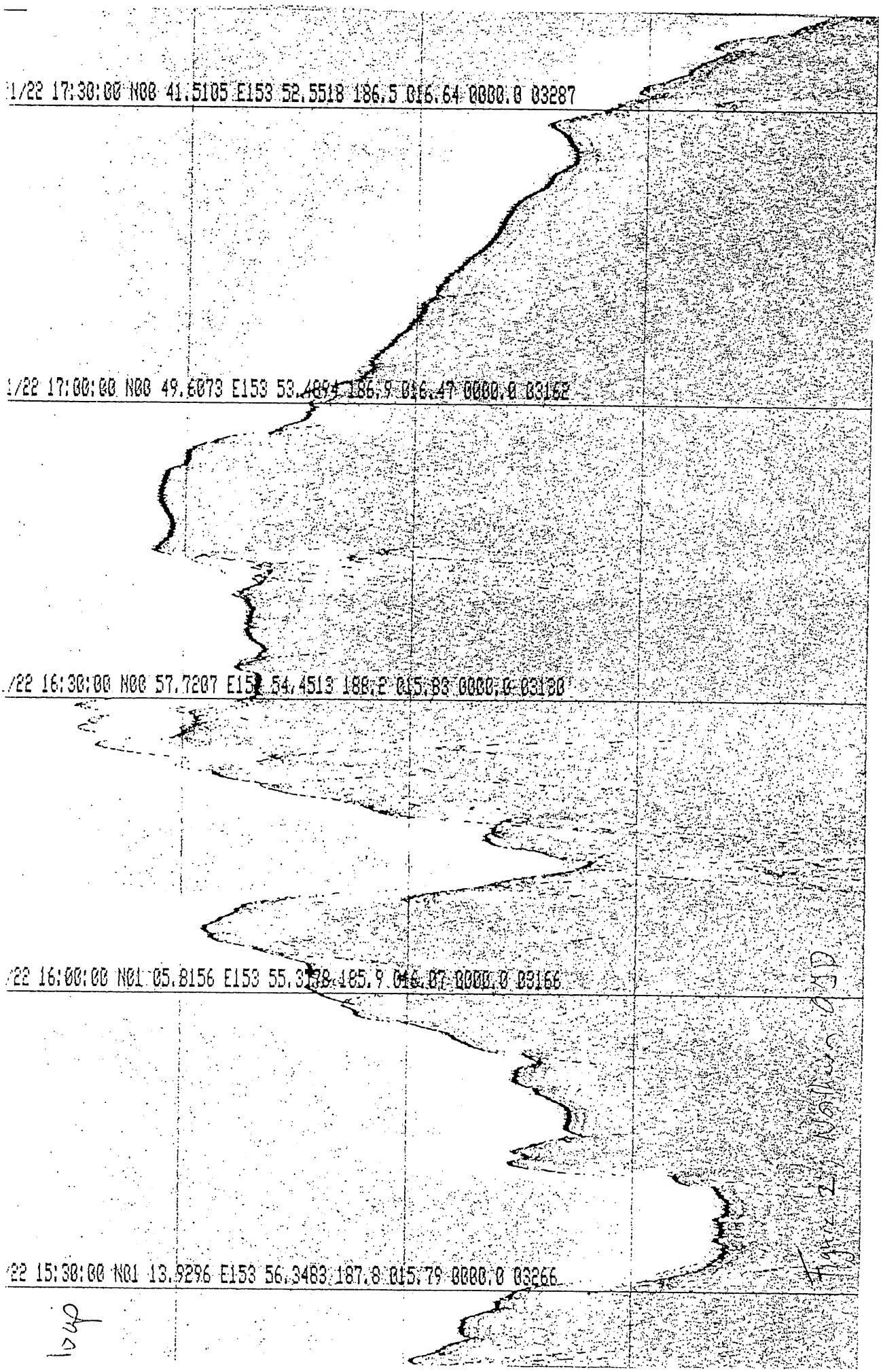
1/22 17:30:00 N00 41.5105 E153 52.5518 186.5 016.64 0000.0 03287
1/22 17:00:00 N00 49.6073 E153 53.4884 186.9 016.47 0000.0 03162
/22 16:30:00 N00 57.7207 E15 54.4513 188.2 015.83 0000.0 03130
/22 16:00:00 N01 05.8156 E153 55.3178 185.9 016.07 0000.0 03166
/22 15:30:00 N01 13.9296 E153 56.3483 187.8 015.79 0000.0 03266

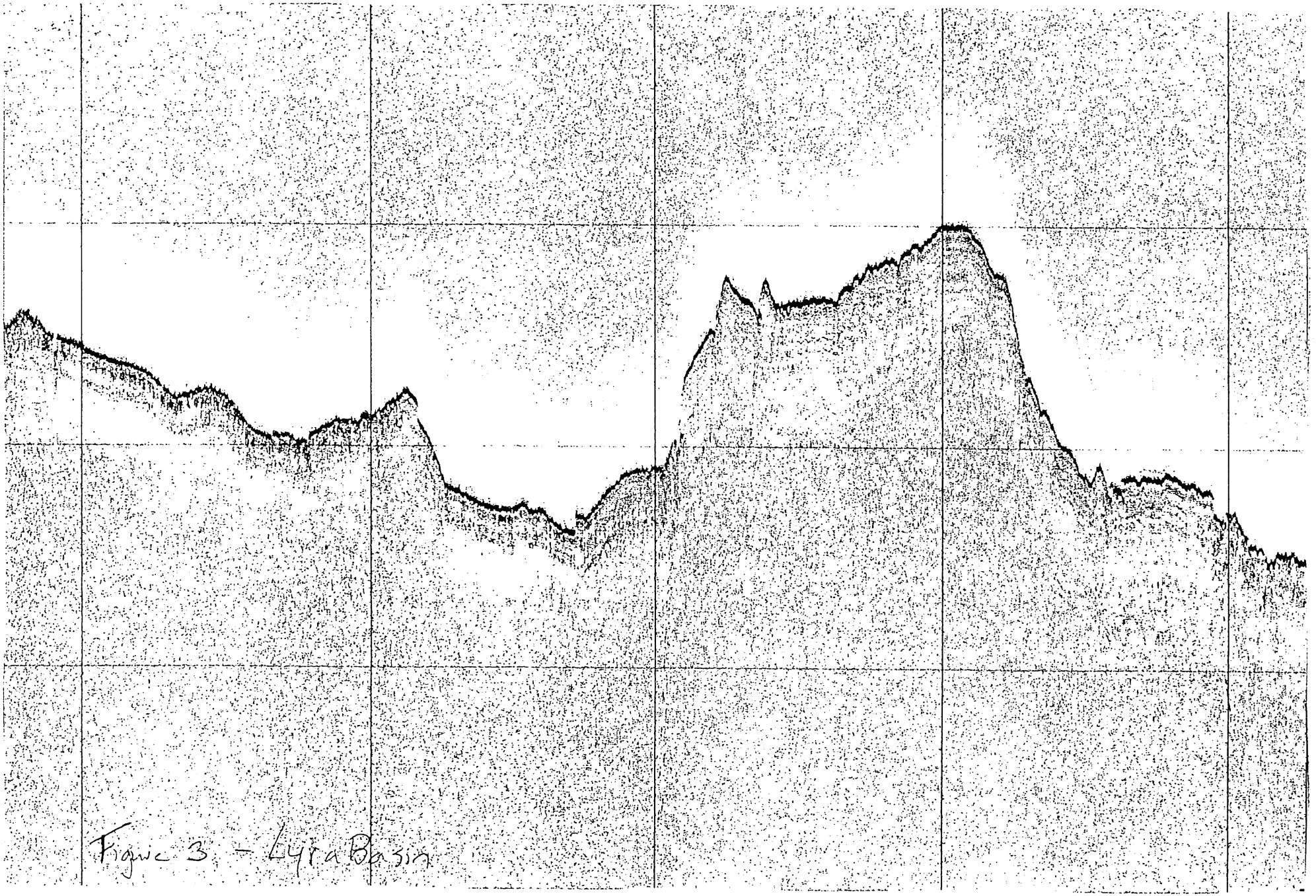

Figure 3 - Lyra Basin

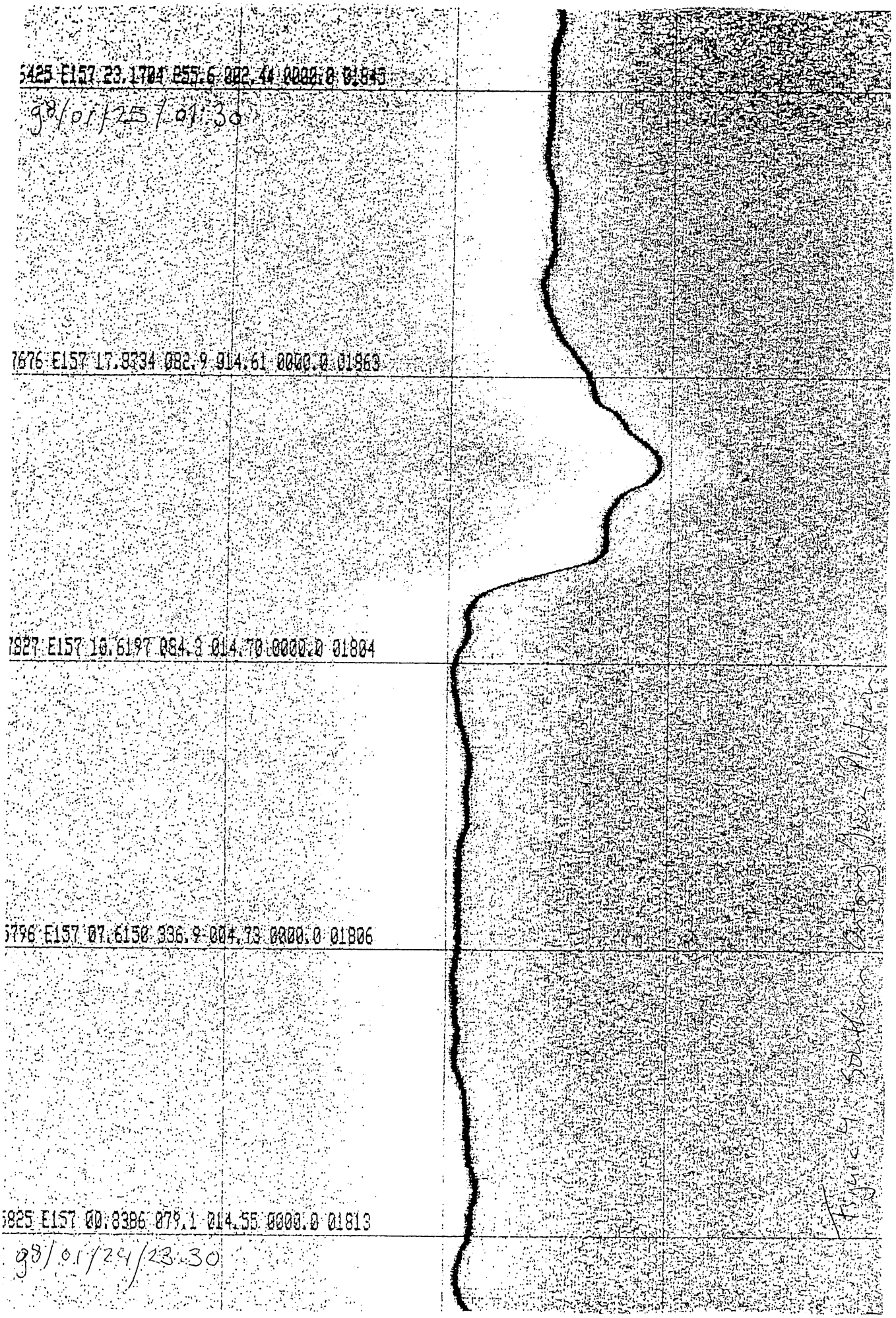
5425 E157 23.1704 855.6 002.44 0000.0 01845
98/01/25/01:30
7676 E157 17.8834 082.9 014.61 0000.0 01863
7827 E157 16.6197 084.3 014.70 0000.0 01804
5796 E157 07.6150 336.9 004.73 0000.0 01806
5825 E157 00.8386 079.1 014.55 0000.0 01813
98/01/24/23:30

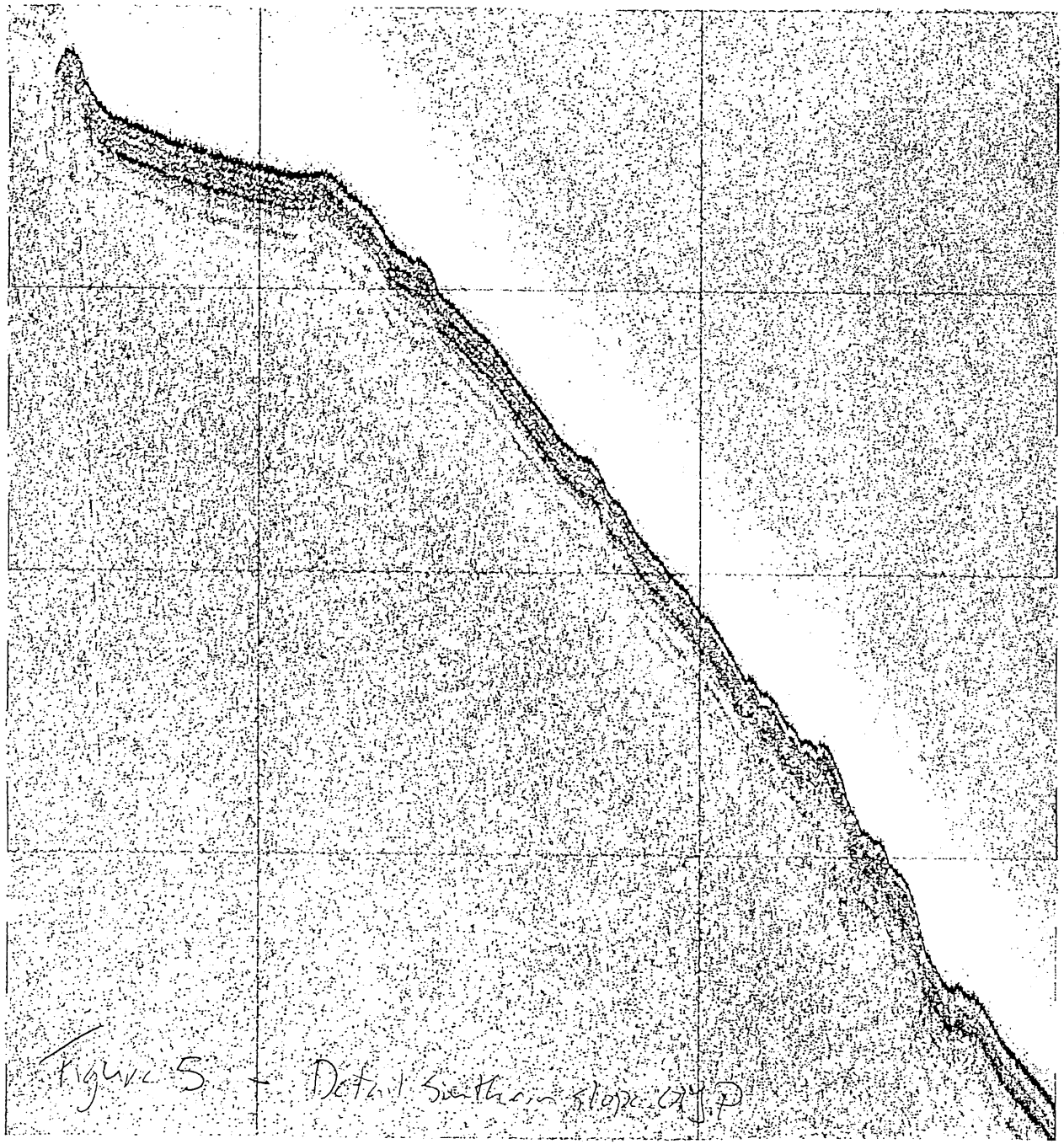

Figure 5 - Detail Seafloor Topography

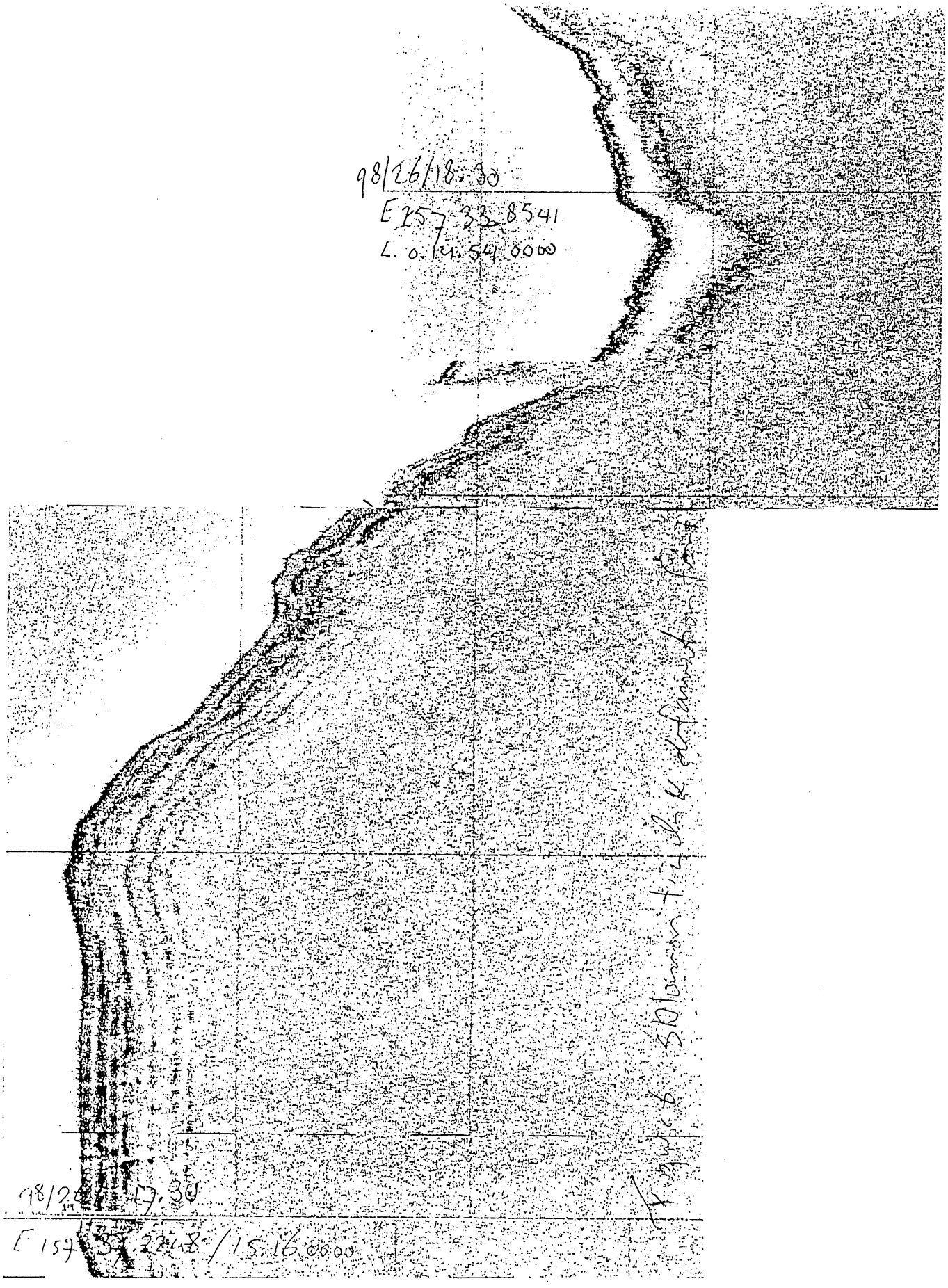
98/26/18:30
E157 33.8541
L. o. 14.54.008
98/2
E 157

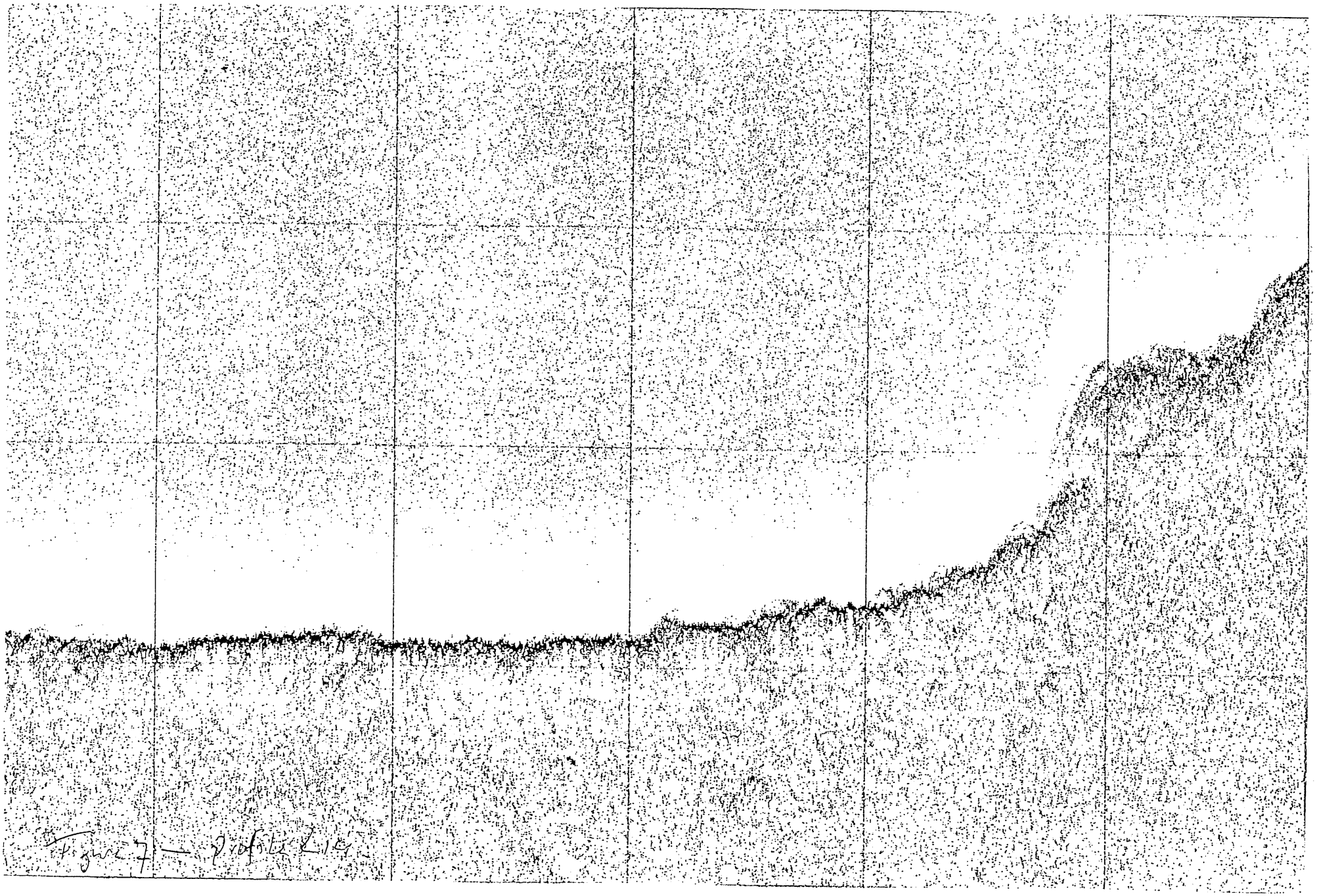

Figure 7 — Profile Line

Figure 8 Line 6 across the thrust front.

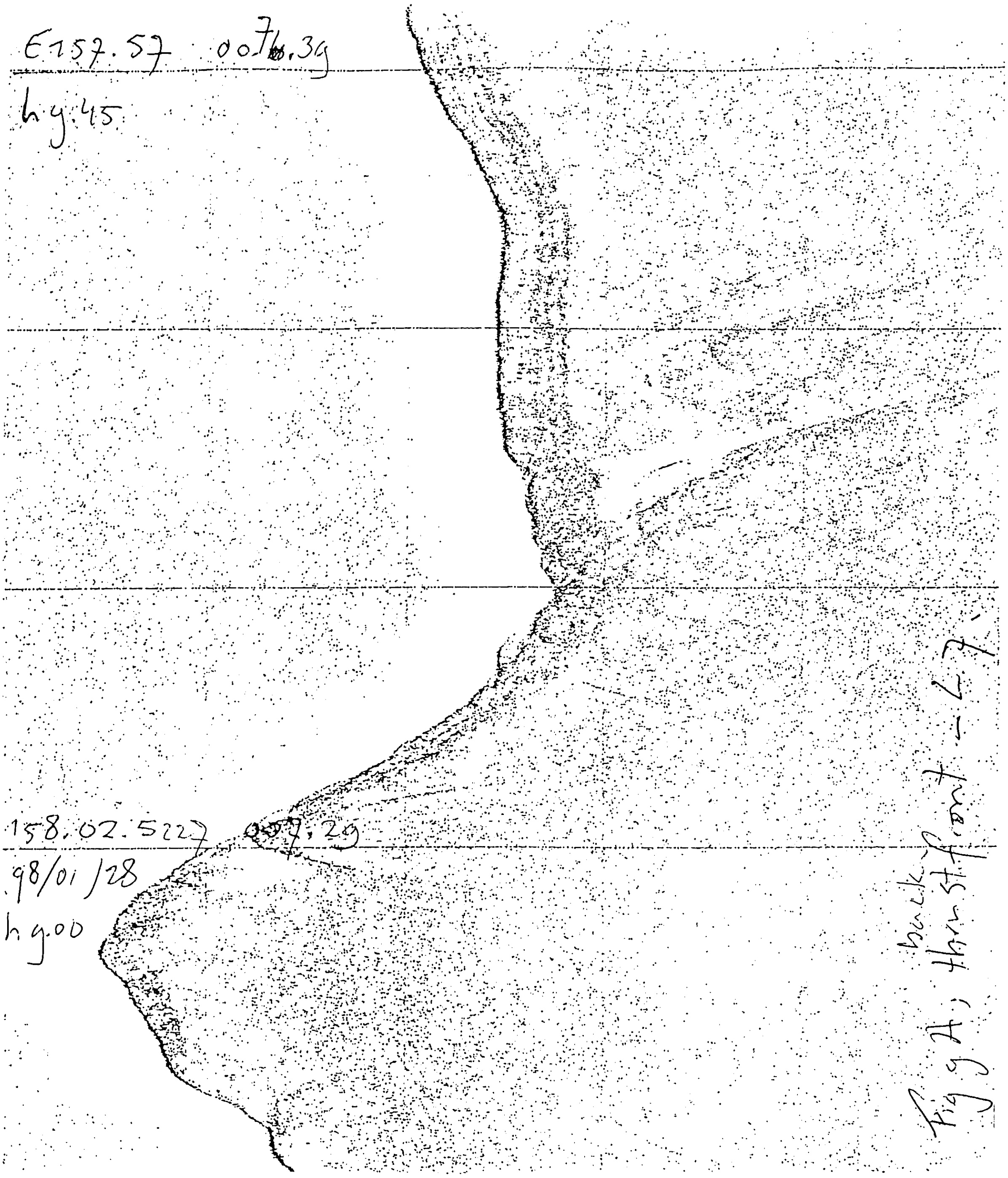

Fig 9 A; back-thrust front

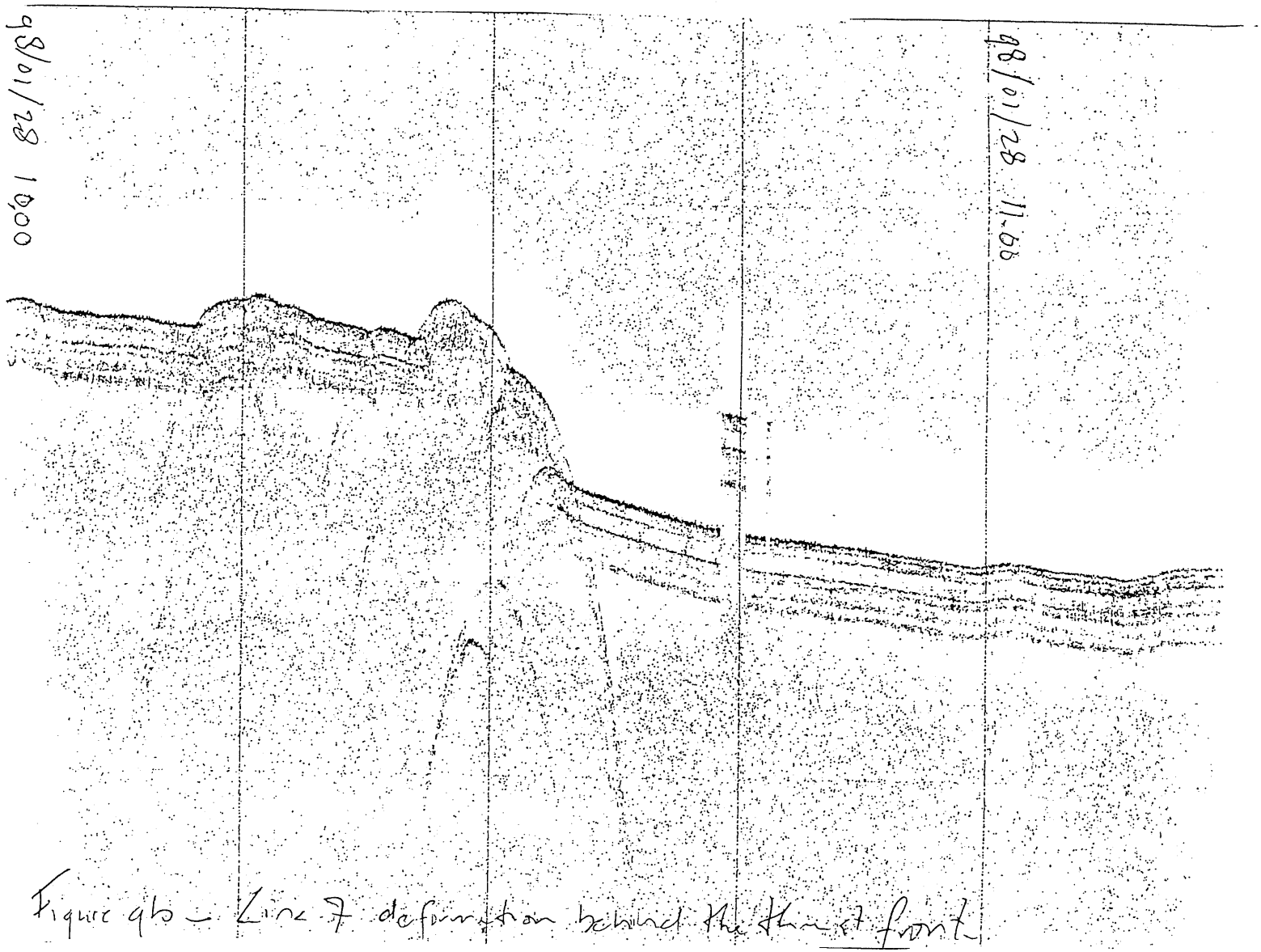

Figure 9b – Line 7 deformation behind the thrust front

98/1/28 20.45

E158 20.665/007.78,

98/01/28 14.15

158.187488/007.55

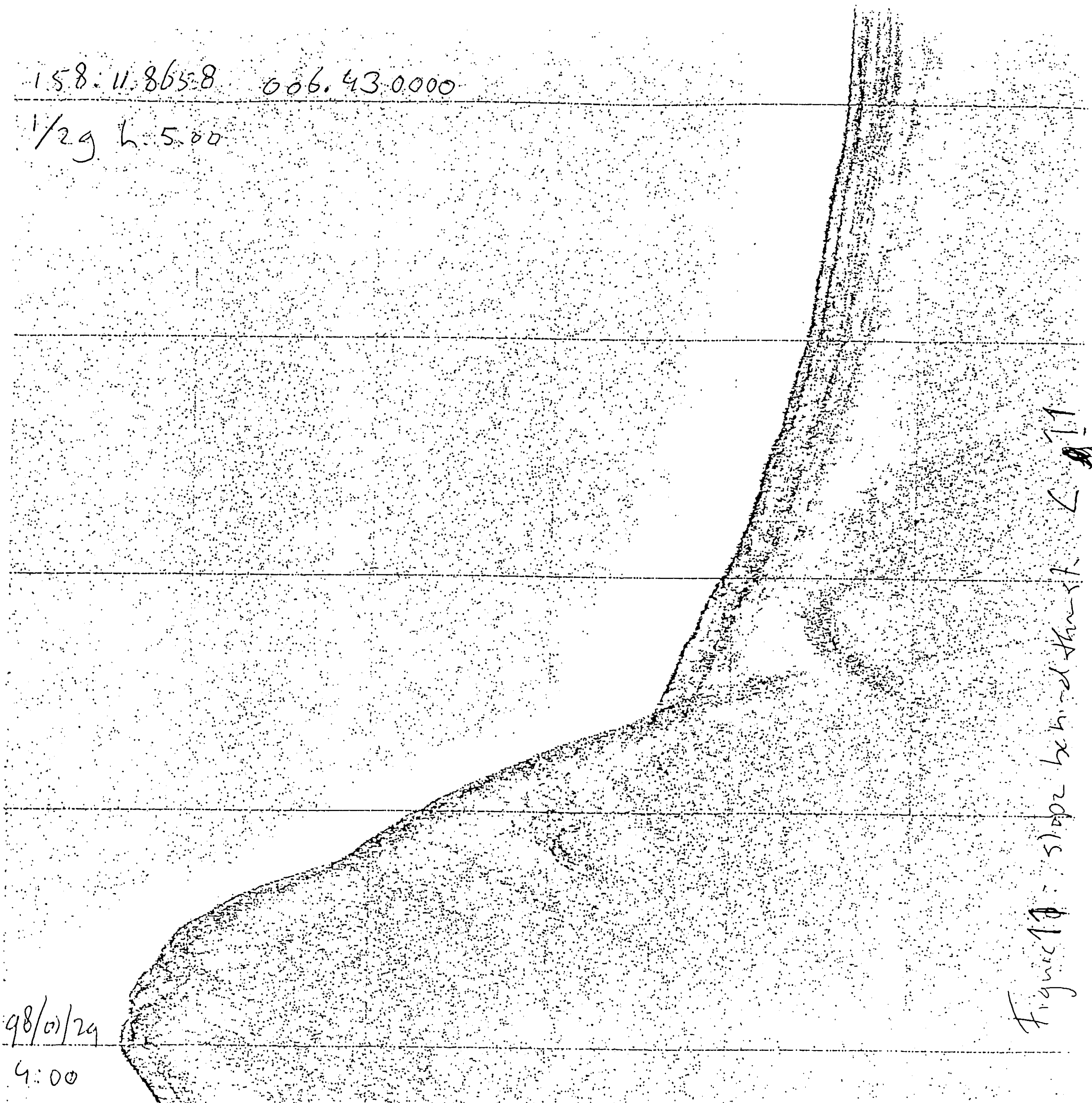

Figure 11: slope behind the rift C 11


98/01/29 10:00
98/01/29 08:45

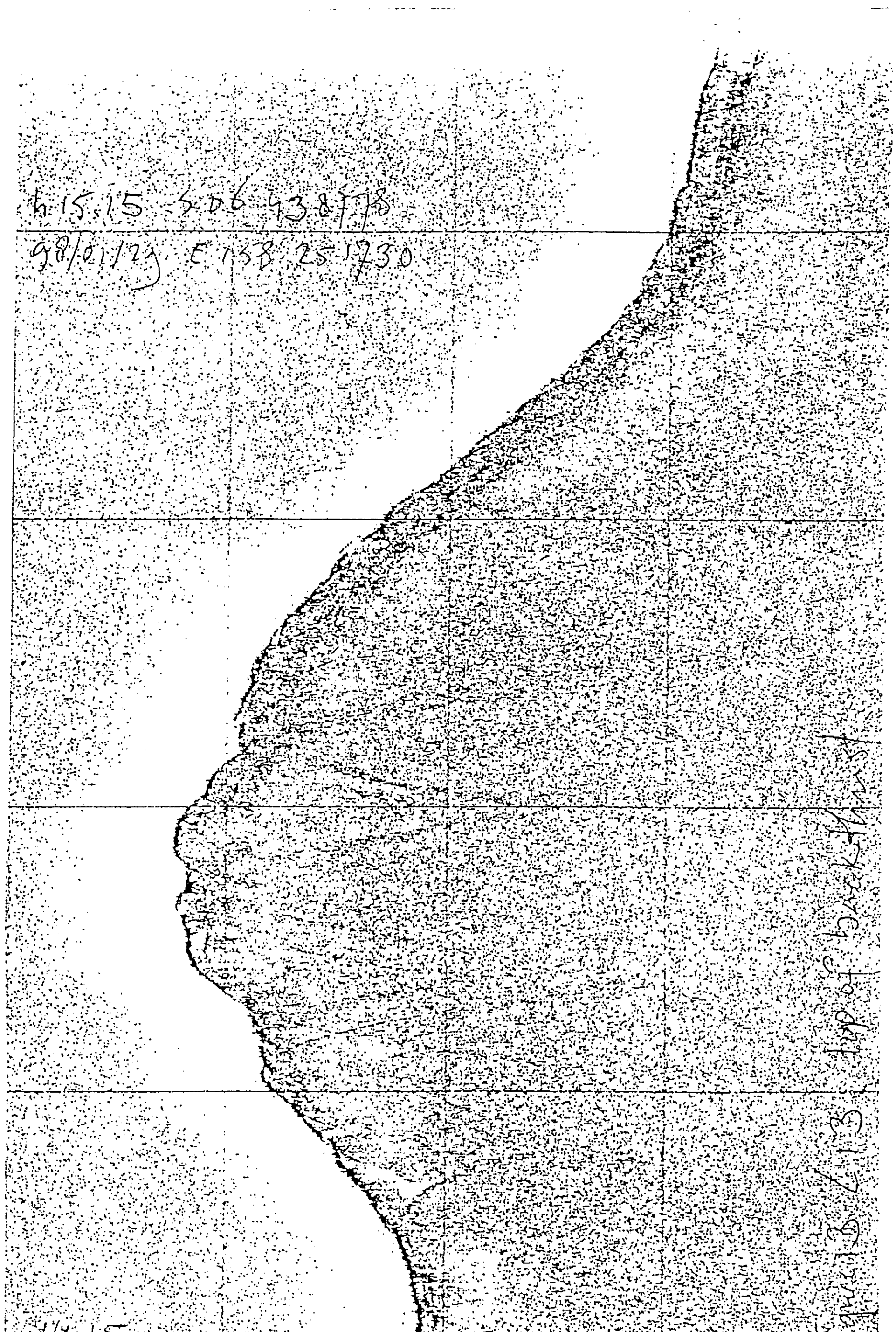

h15.15 S06 43.8778
98/01/29 E 158 25.1730
14.15
158 33.2280
98/01/29 S09 40.8547

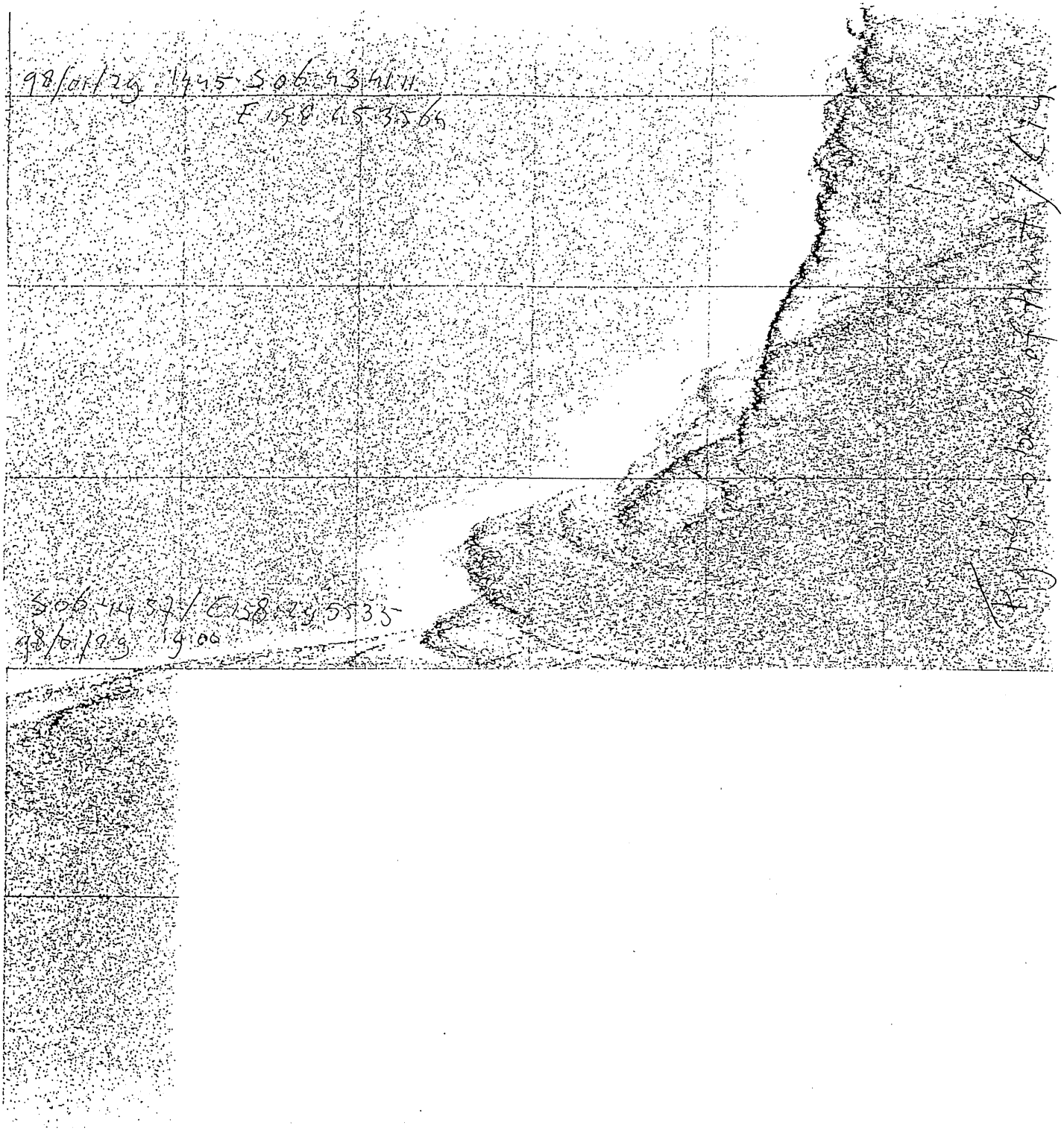
98/ar/24 1445 506 934 11
E 158 45 3566
506 44 94 / E 158 25 5533
98/6/29 1900

Figure 15 - L15.

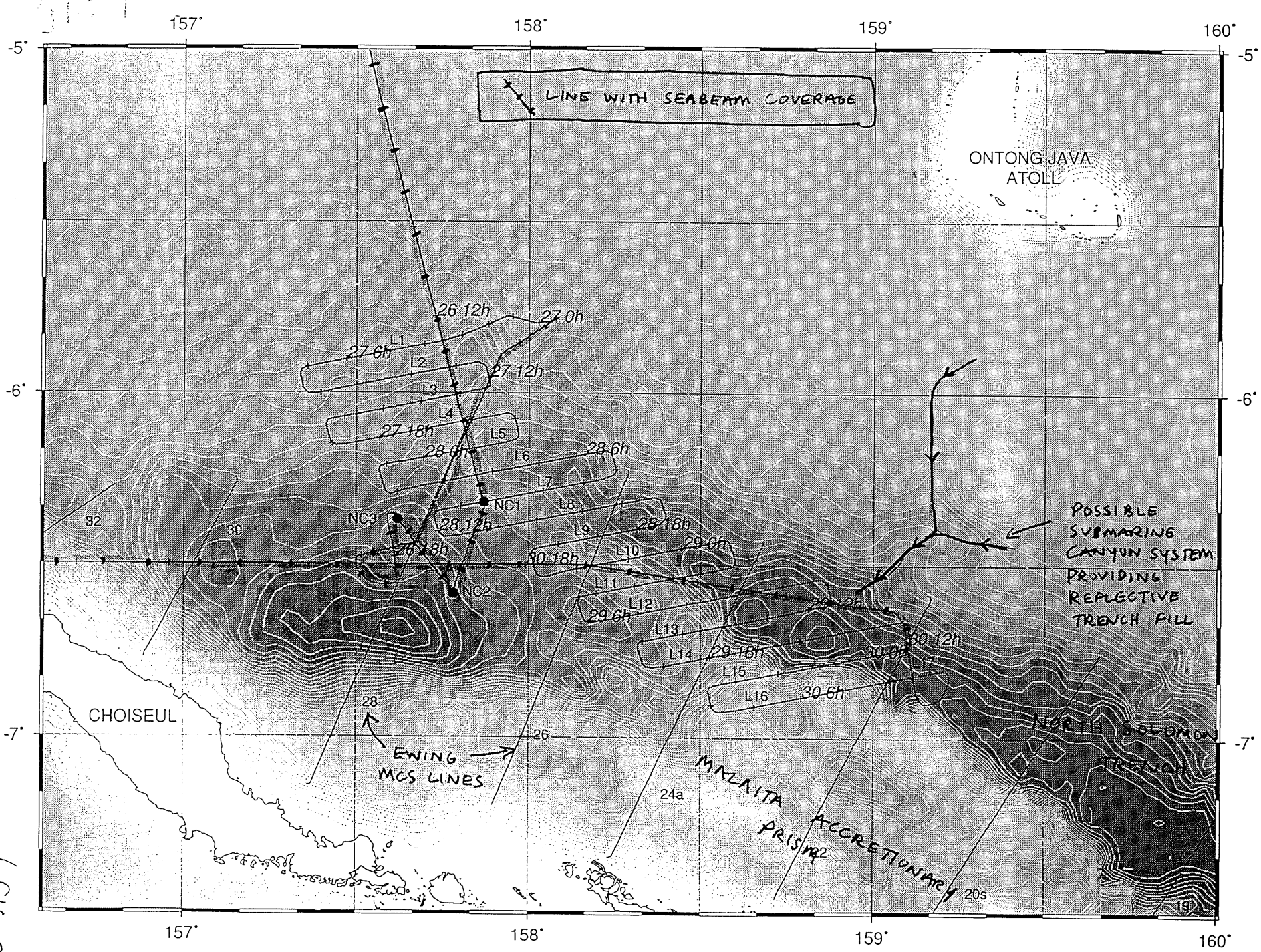
157°
158°
159°
160°
-5°
-6°
-7°
LINE WITH SEABEAM COVERAGE
ONTONG JAVA ATOLL
26 12h
27 0h
27 6h
27 12h
27 18h
28 0h
28 6h
28 12h
28 18h
29 0h
29 6h
29 12h
29 18h
30 0h
30 6h
30 12h
30 18h
L1
L2
L3
L4
L5
L6
L7
L8
L9
L10
L11
L12
L13
L14
L15
L16
NC1
NC2
NC3
32
30
28
26
24a
20s
19
POSSIBLE SUBMARINE CANYON SYSTEM PROVIDING REFLECTIVE TRENCH FILL
CHOISEUL
EWING MCS LINES
MALAITA ACCRETIONARY PRISM
NORTH SOLOMONS TRENCH

(Fig. 2)